Observational constraints on the abundance of Primordial Black Holes (PBHs)

Anne Green

University of Nottingham, UK

1. (selected) new/updated constraints
2. Effect of PBH distribution on LMC microlensing constraints
3. How open is the asteroid mass window?

1. (selected) new/updated constraints

- OGLE long duration LMC microlensing
- supermagnified stars
- flux ratios of multiply lensed quasars

Compilation of observational constraints

(under ‘standard’ assumptions, including a delta-function PBH mass function)

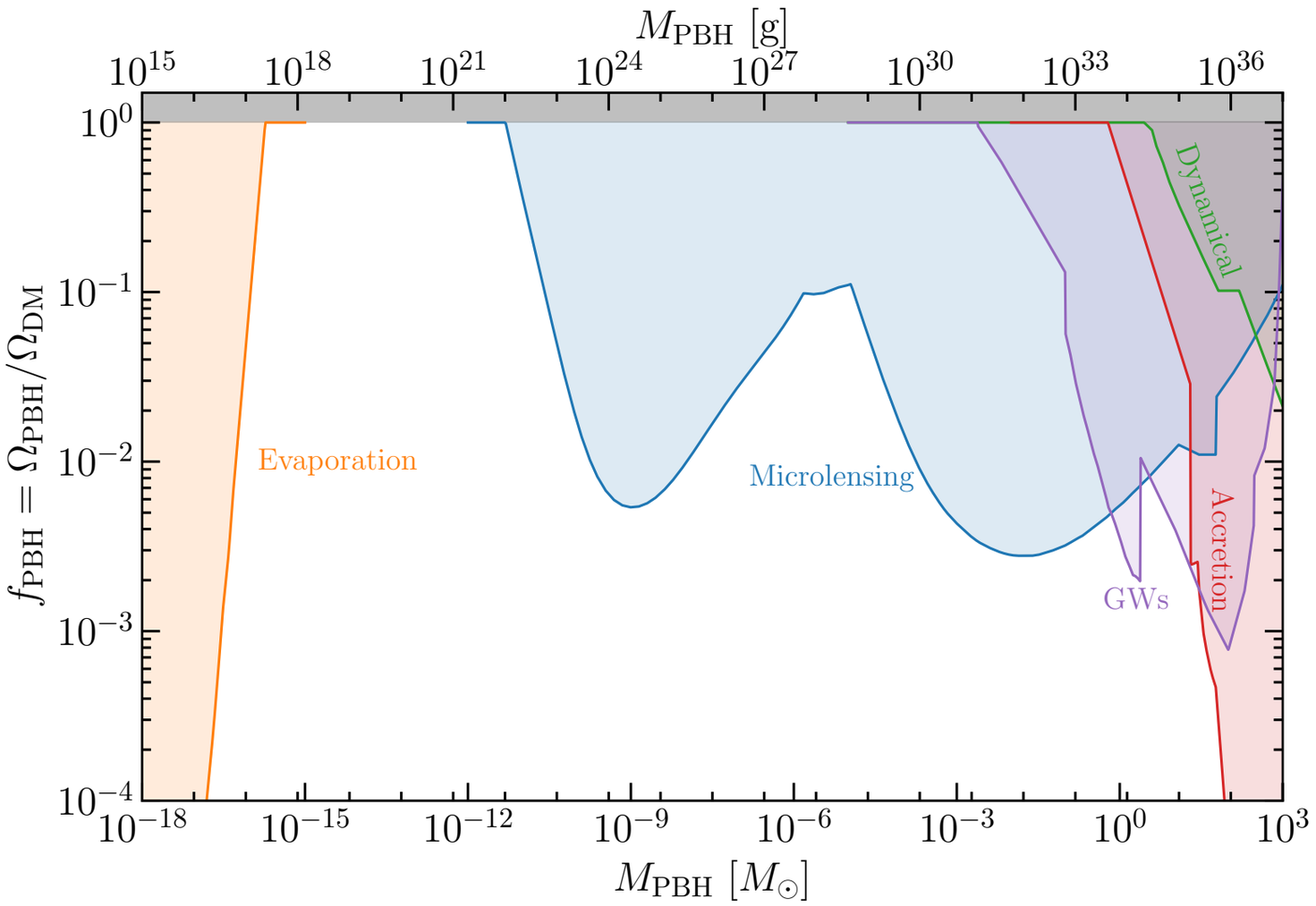

evaporation

lensing

gravitational waves

accretion

dynamical

https://github.com/bradkav/PBHbounds

OGLE long-duration LMC microlensing

Stellar microlensing: temporary (achromatic) brightening of background star when compact object passes close to the line of sight. Paczynski

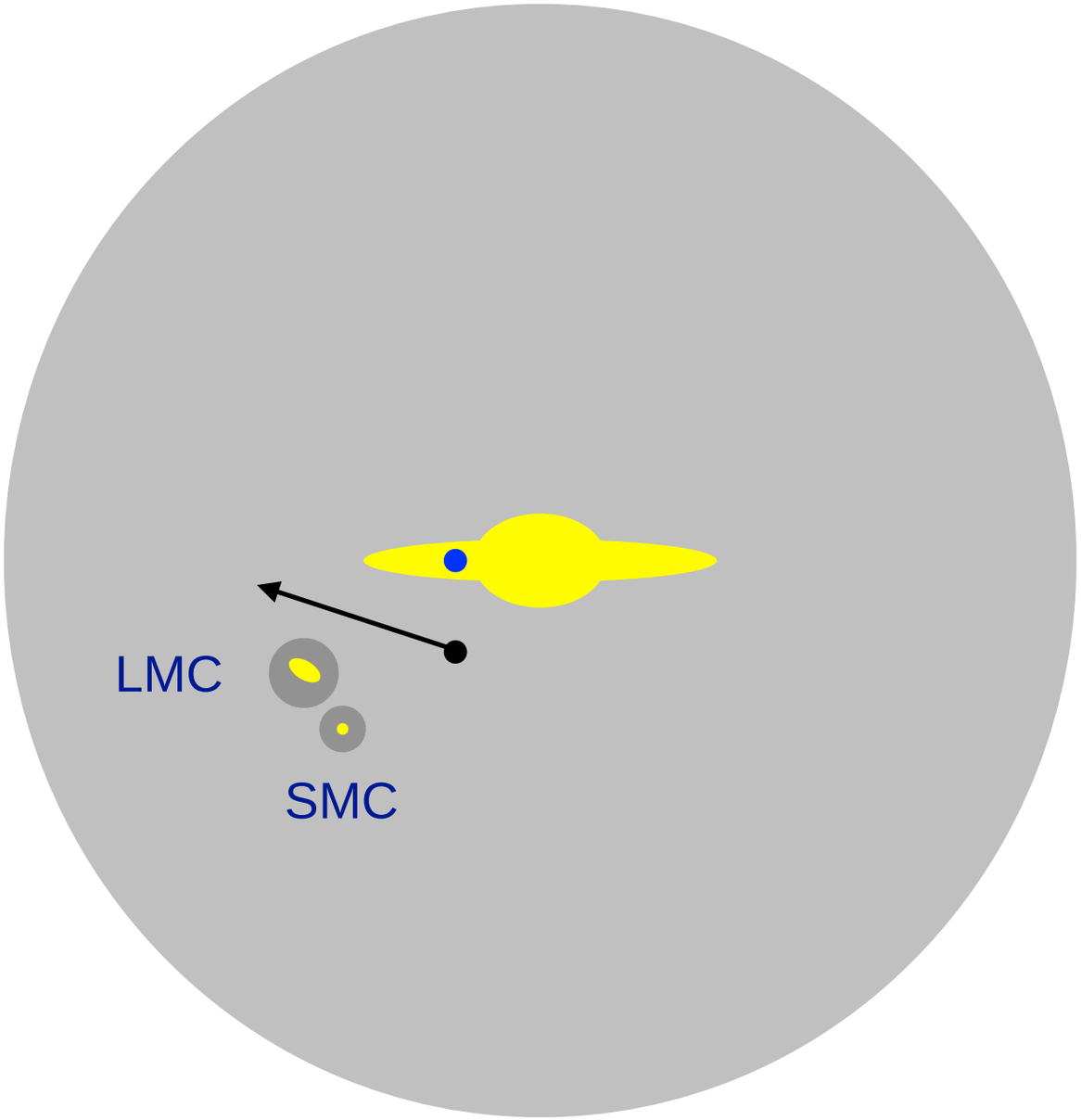

Not to scale!

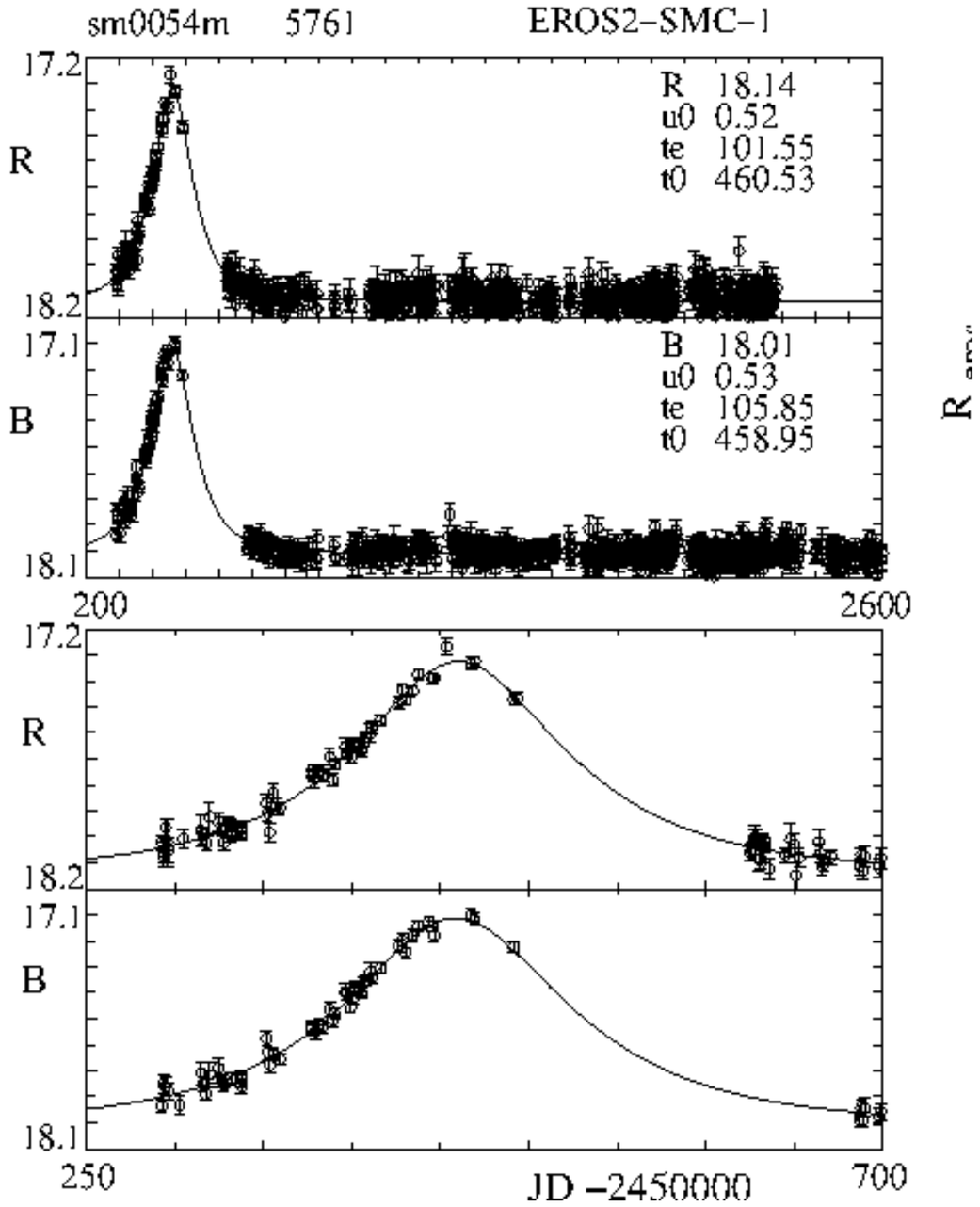

EROS

Einstein radius:

$$R_{\rm E}(x) = 2\left[\frac{GMx(1-x)D_{\rm s}}{c^2}\right]^{1/2} \approx 3\times10^{-4}\,{\rm pc}\,\sqrt{x(1-x)}\left(\frac{M}{10M_\odot}\right)^{1/2}\left(\frac{D_{\rm s}}{50\,{\rm kpc}}\right)^{1/2}$$

x = fractional distance along line of sight

along the line of sight

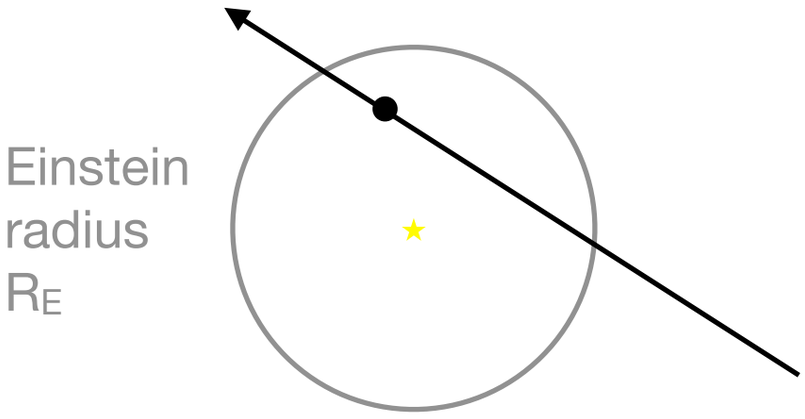

perpendicular to the line of sight

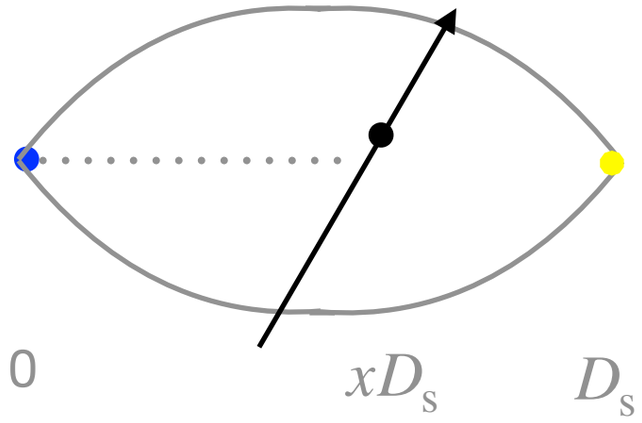

'Duration' of event (Einstein diameter crossing time):

$$\hat{t} = \frac{2R_E}{v} \approx 3\,{\rm yr}\sqrt{x(1-x)}\left(\frac{M}{10M_\odot}\right)^{1/2}\left(\frac{D_s}{50\,{\rm kpc}}\right)^{1/2}\left(\frac{v}{200\,{\rm km\,s^{-1}}}\right)^{-1}$$

Constraints on planetary and stellar mass PBHs from 20 years of OGLE LMC microlensing observations: Mroz et al. arXiv:2403.02386

Observed 13 events with duration (Einstein radius crossing time) <1 year, no longer duration events.

Expect ~6 events from stars in LMC and ~(7-15) from stars in MW disk.

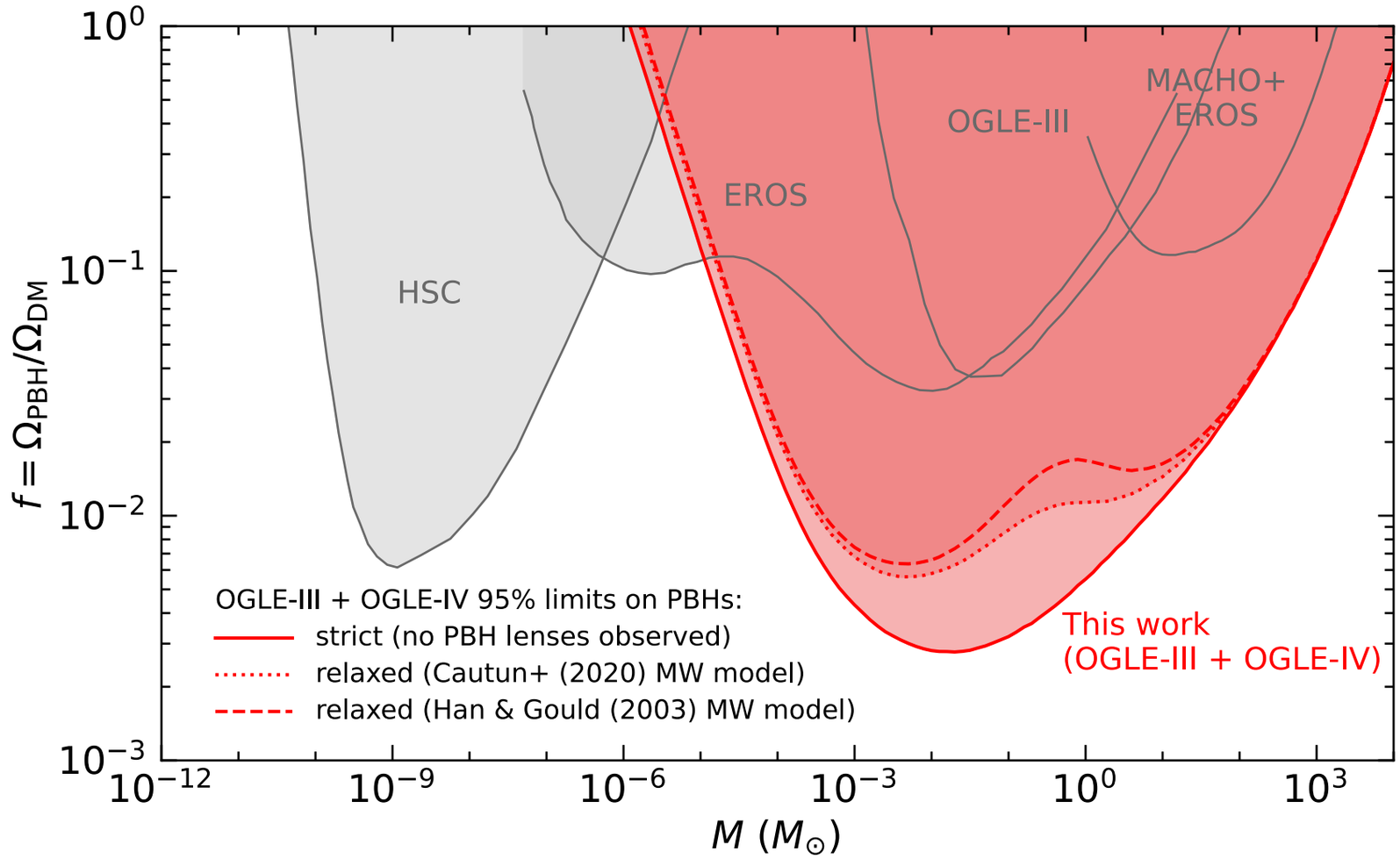

_____ strict (assumes all 13 events are due to stars/stellar remnants in LMC or MW disk)

…. & - - - - allow contribution from MW halo (2 different models for MW disk)

Supermagnified stars

When a distant star crosses a galaxy cluster caustic get huge magnification which can be increased by microlensing by compact objects (stars, stellar remnants, dark compact objects,..) in cluster. Miralda-Escude.

However if large fraction of DM is in compact objects magnification is reduced.

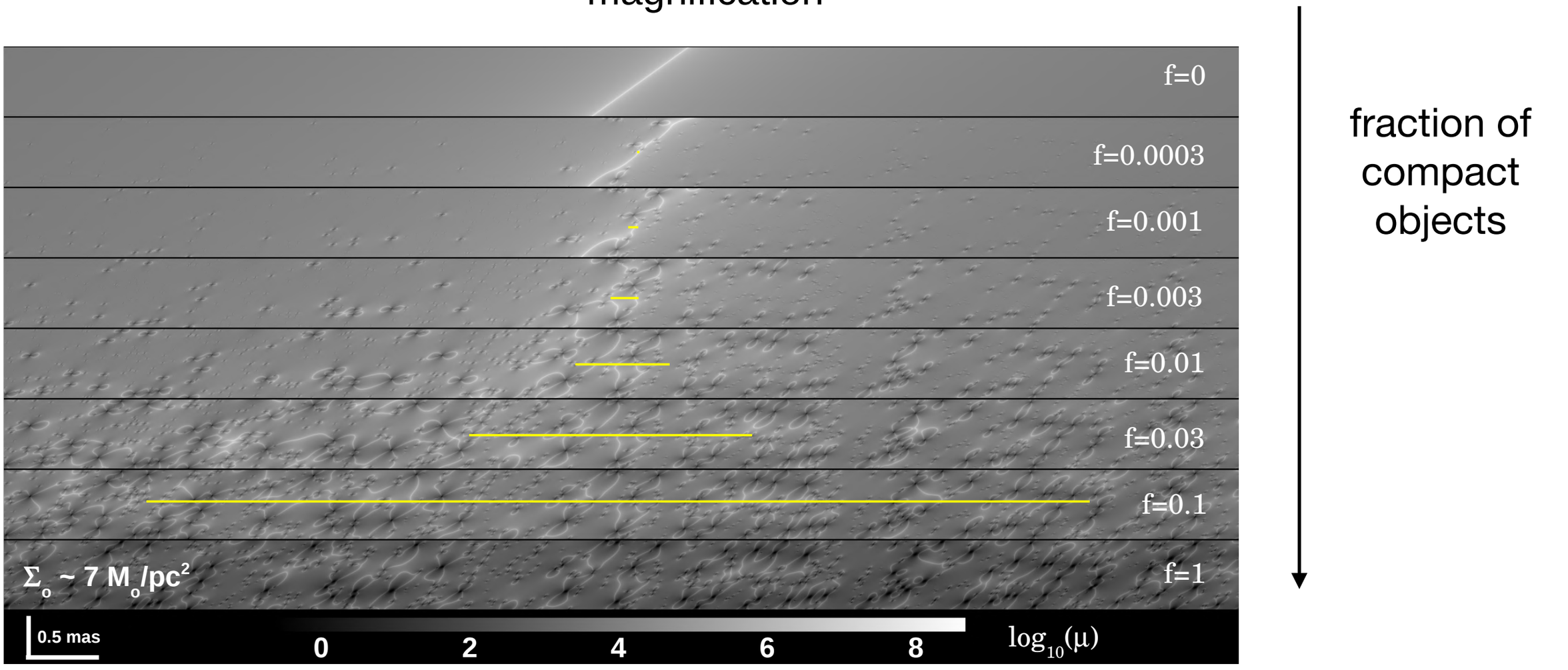

Kelly et al.

Supermagnified stars

When a distant star crosses a galaxy cluster caustic get huge magnification which can be increased by microlensing by compact objects (stars, stellar remnants, dark compact objects,..) in cluster. Miralda-Escude.

However if large fraction of DM is in compact objects magnification is reduced.

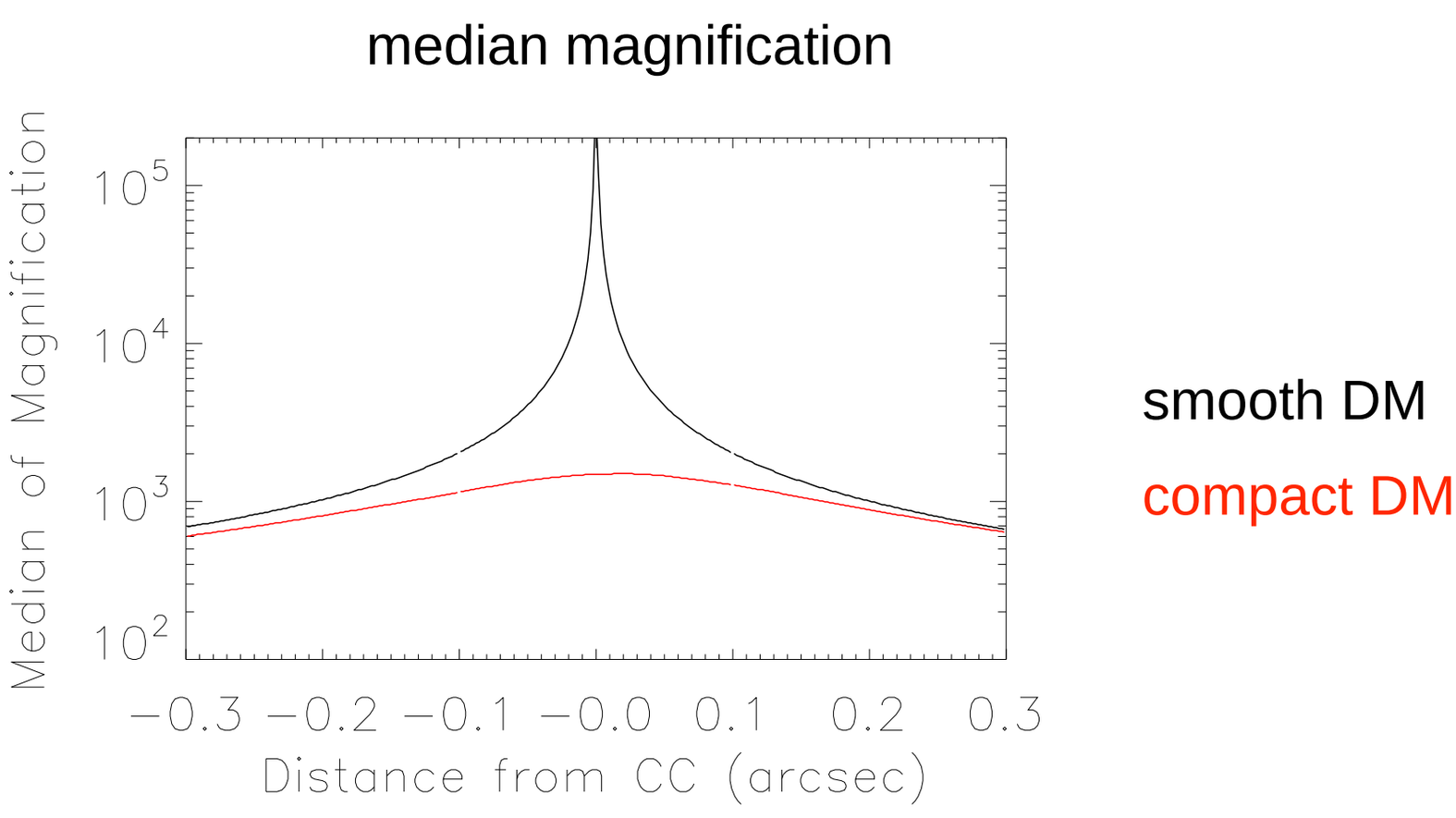

Kelly et al.

Icarus: star at red-shift 1.5, magnified x2000!, discovered serendipitously.

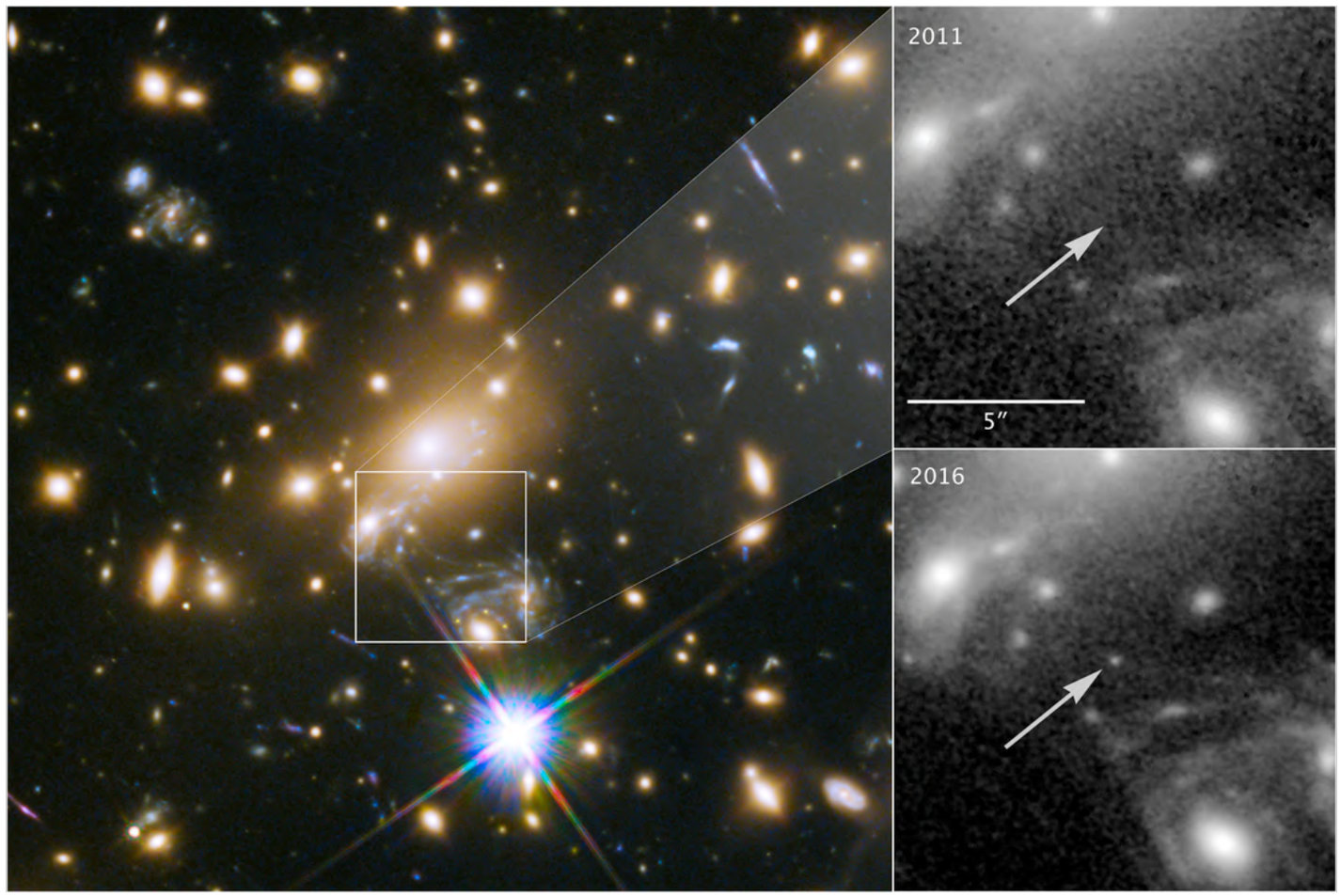

Kelly et al.

From positions of images of 9 supermagnified stars (Icarus, Warhol, Earendel, Mothra (at z=2.1),…): planetary mass and heavier compact objects make up less than ~3% of the dark matter. Vall Müller & Miradla-Escudé arXiv:2403.16989

Flux ratios of multiply-lensed quasars

Microlensing by compact objects in the lens galaxy leads to variations variation in the brightness of multiple-image quasars. Chang and Refsdal

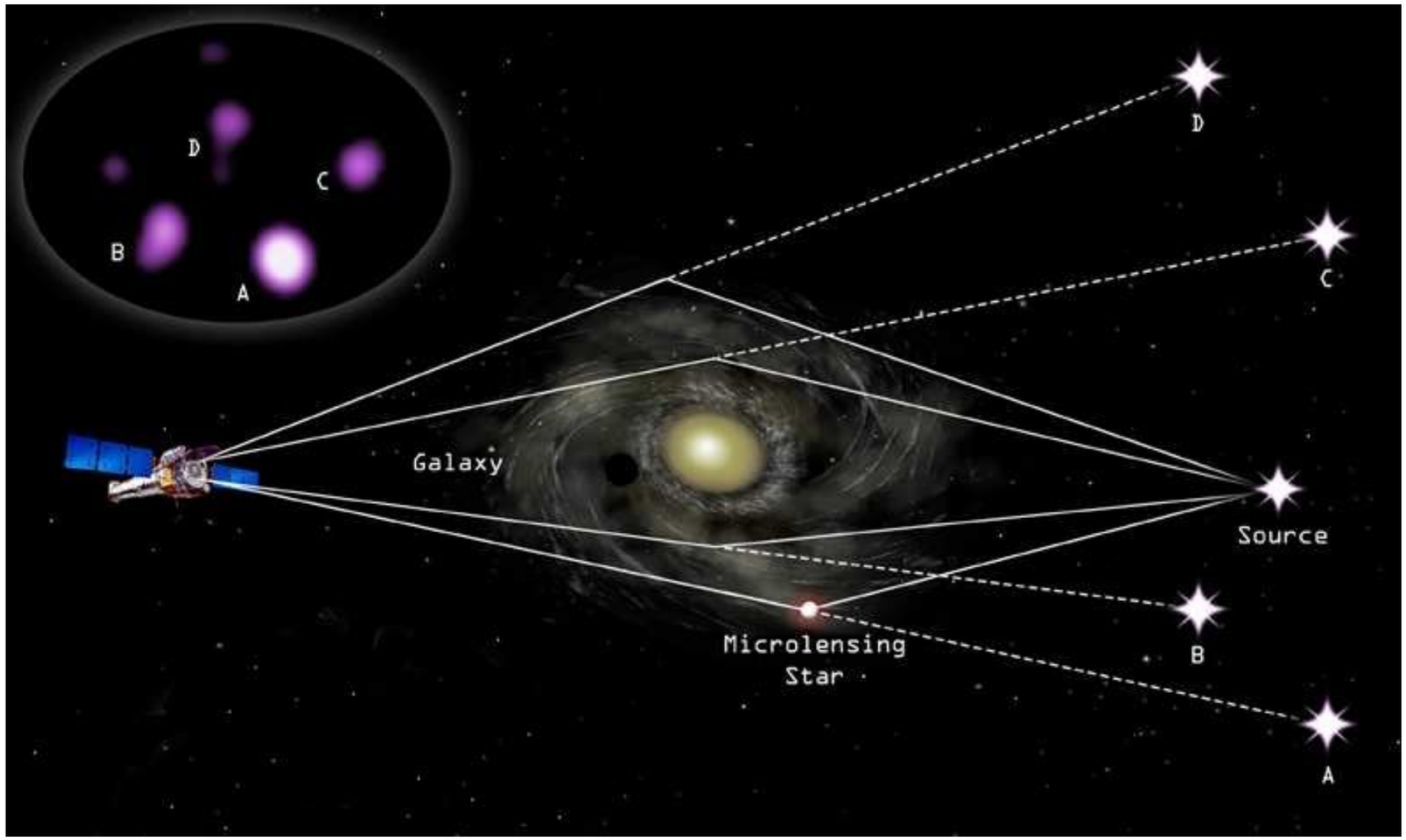

Anguita

Flux ratios of multiply-lensed quasars

Microlensing by compact objects in the lens galaxy leads to variations variation in the brightness of multiple-image quasars. Chang and Refsdal

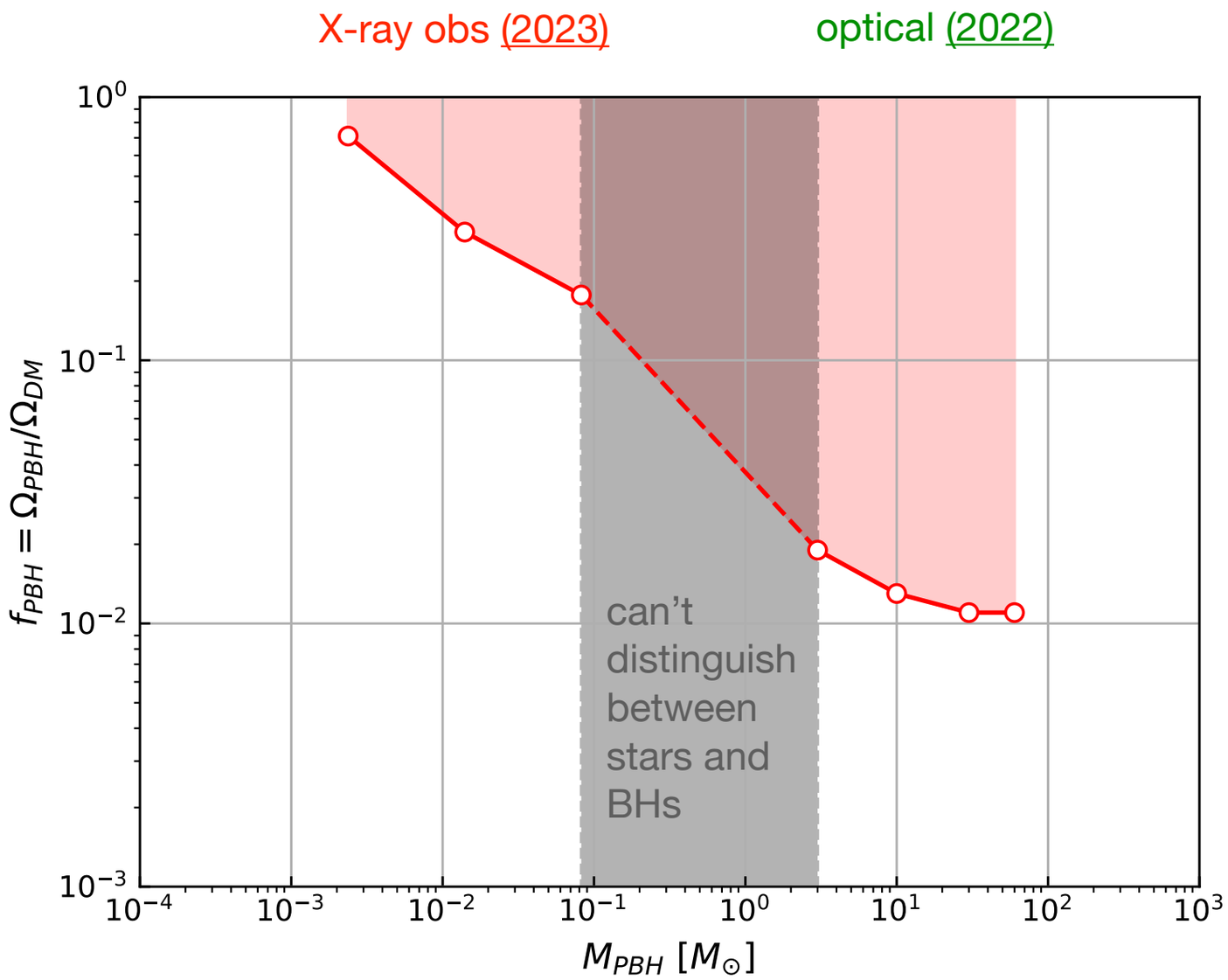

Esteban-Gutierrez et al. (2023)

Compilation of observational constraints

(under ‘standard’ assumptions, including a delta-function PBH mass function)

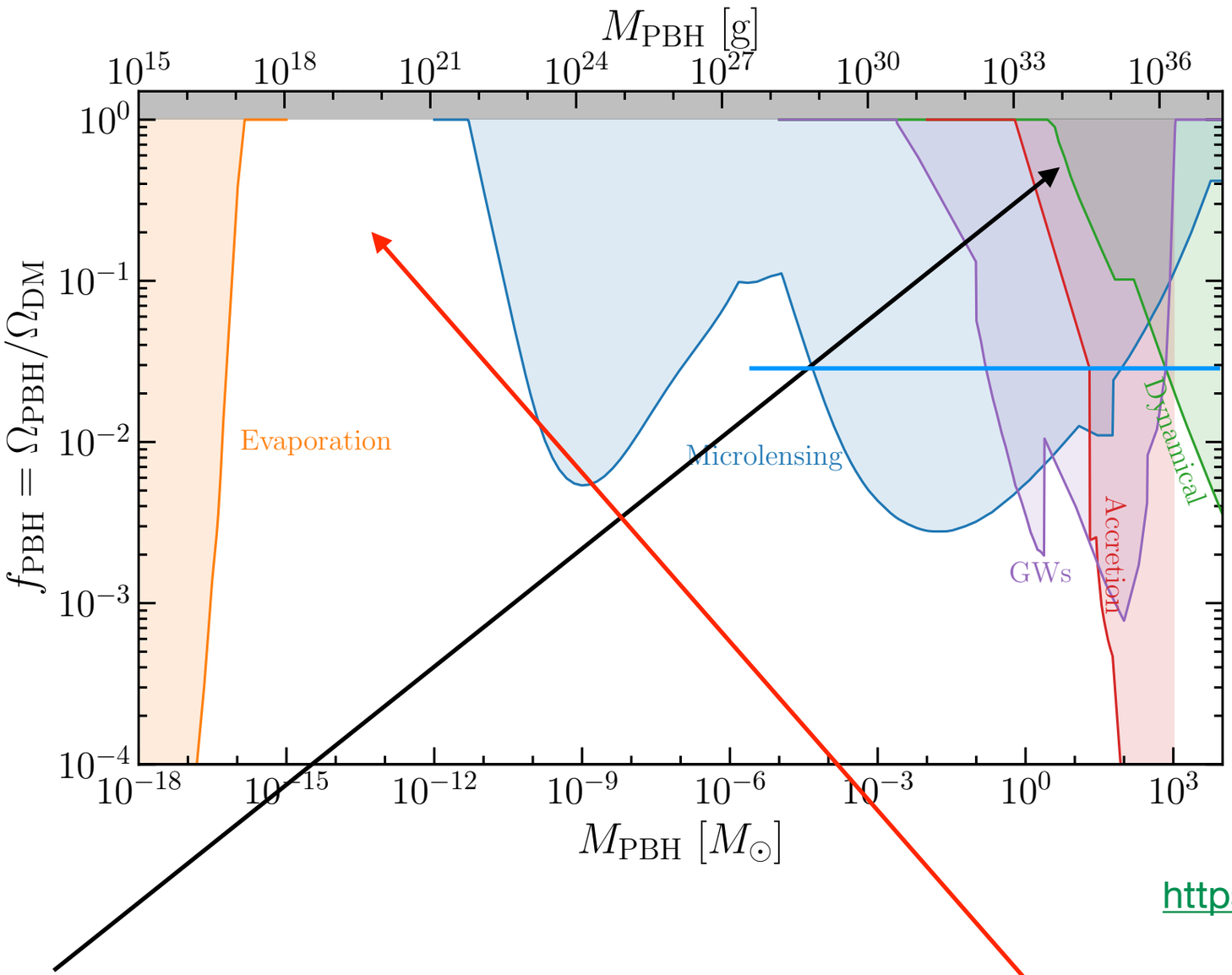

evaporation

lensing

gravitational waves

accretion

dynamical

https://github.com/bradkav/PBHbounds

multi-Solar mass PBH making up all of the DM is excluded.

However there is a hard to probe, open window for very light (asteroid mass) PBHs.

2. Effect of PBH distribution on LMC microlensing constraints

- Clustering
- MW density profile

LMC microlensing constraints: clustering

Due to Poisson fluctuations in PBH distribution, PBH clusters form shortly after matter-radiation equality. Afshordi, Macdonald & Spergel; Inman & Ali-Haïmoud; Jedamzik

distribution at $z = 99$

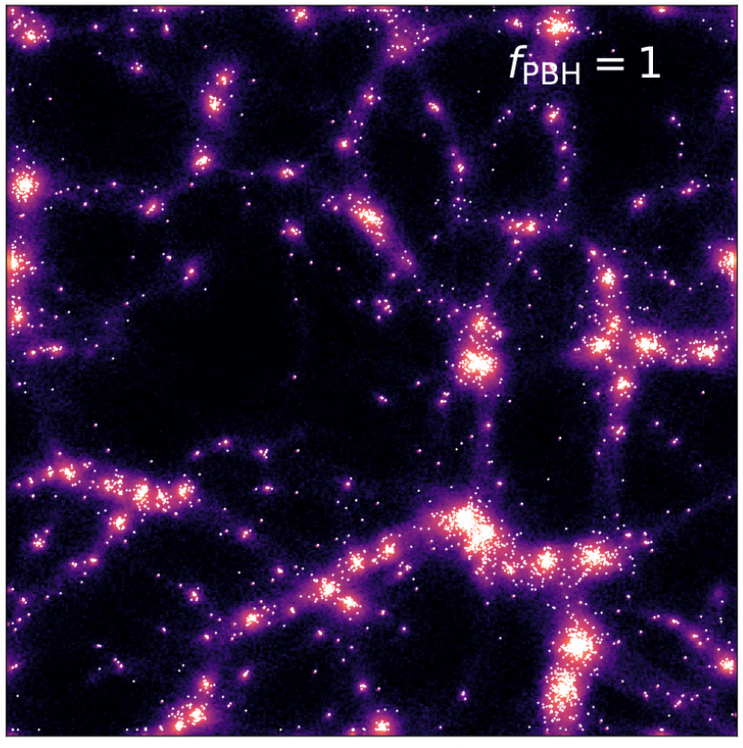

Inman & Ali-Haïmoud

Clusters containing a small number of PBHs, $N_{\rm cl}$, are most common, but those with $N_{\rm cl} \lesssim 10^3$ will evaporate by present day.

Clusters formed from gaussian perturbations are sufficiently extended that PBHs act as lenses indvidually (rather than the cluster as a whole). Petaĉ, Lavalle & Jedamzik; Gorton & Green

LMC microlensing differential event rate for clustered DM and standard smooth DM

all DM in clusters containing $N_{\rm cl} = 10^6$ PBHs

n.b. extremely unrealistic!

$M_{\rm PBH} = 1 M_\odot$

$M_{\rm PBH} = 10 M_\odot$

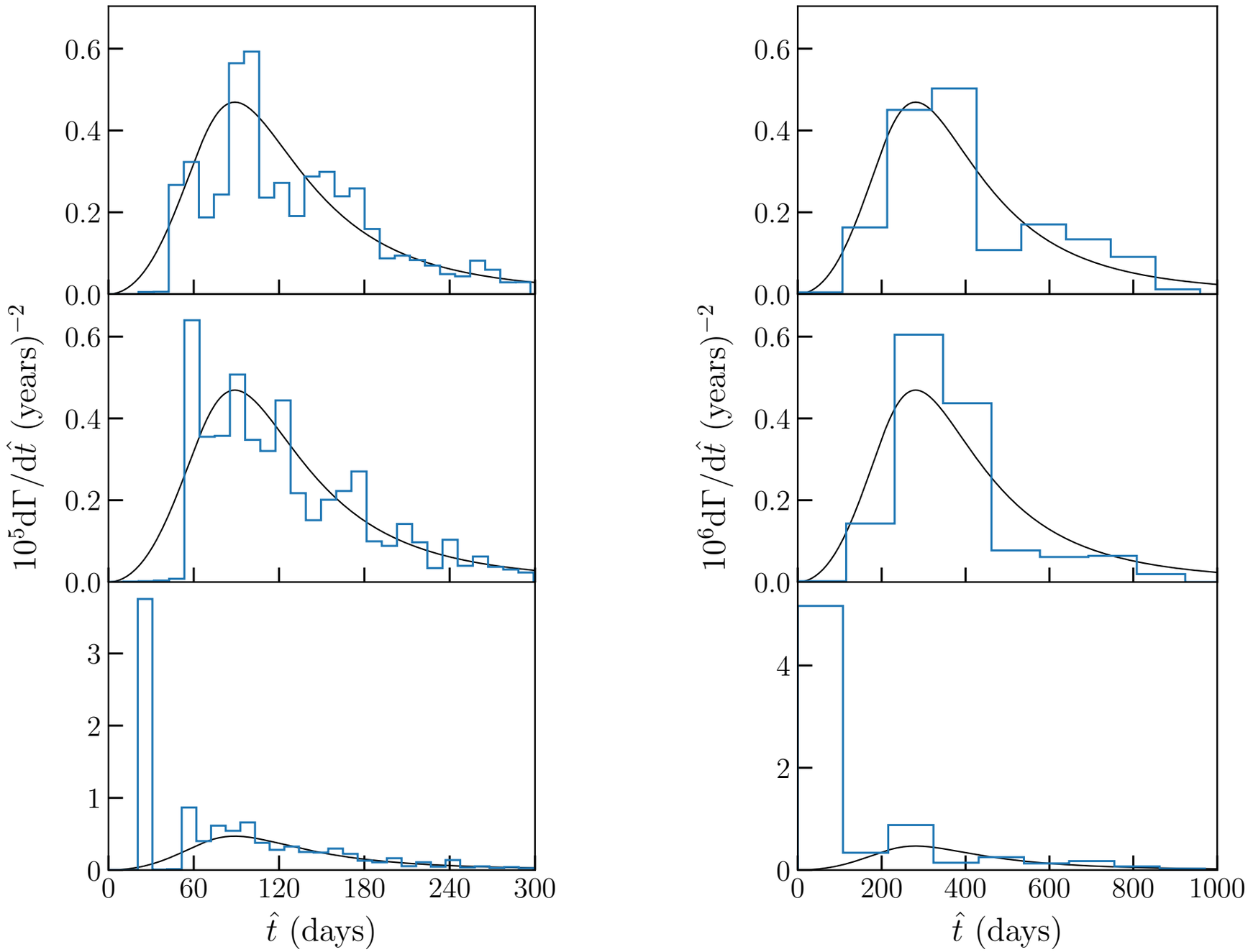

Typical realisations

No close cluster.
Deficit of short duration events.

Rare realisation

Close cluster.
Excess of short duration events.

Probability distribution of number of events in a long-duration microlensing survey if all of the DM is in PBHs clusters containing $N_{\rm cl}$ PBHs with mass $M_{\rm PBH} = 10^3 M_\odot$

Typical realisations

No close cluster.
Deficit of events.

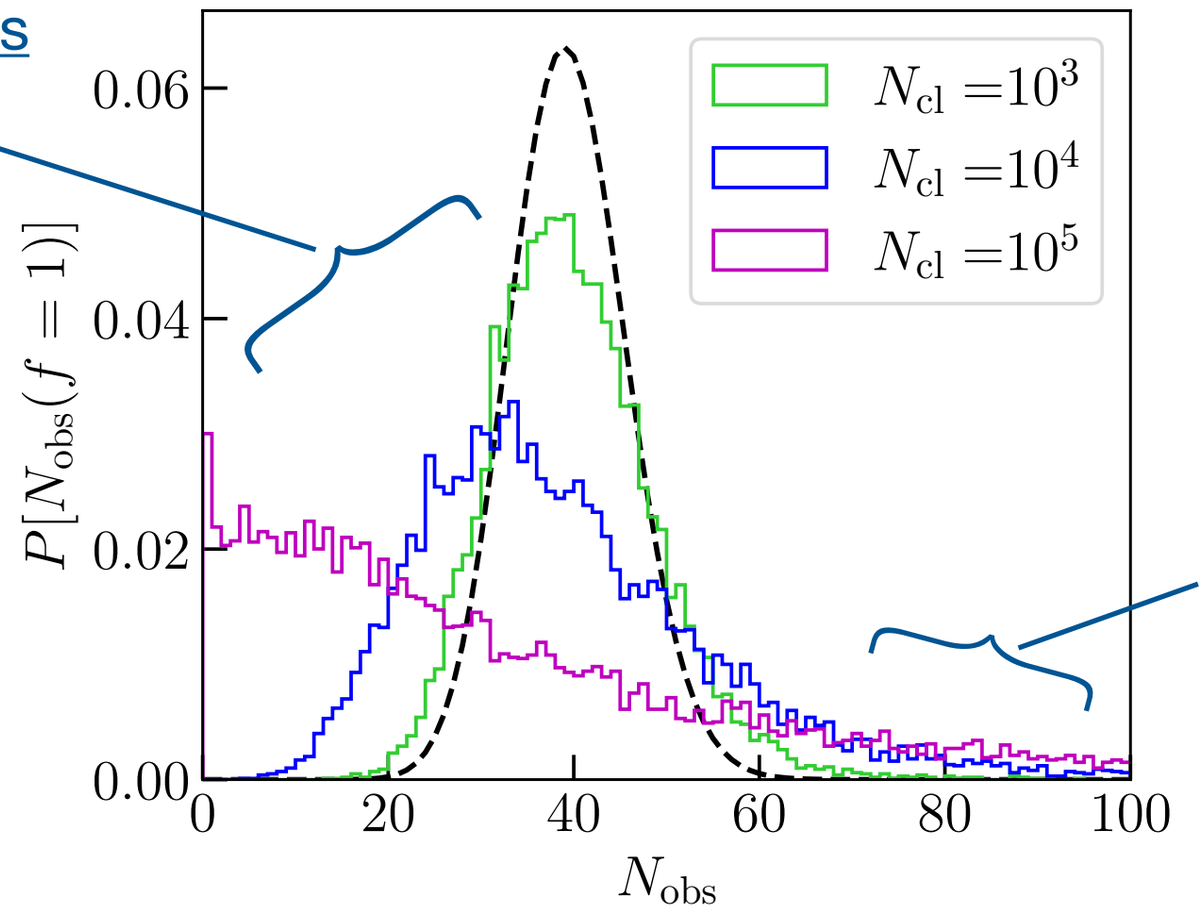

Rare realisations

Close cluster.
Excess of events.

Change in constraints is negligible apart (possibly) from at largest $M_{\rm PBH}$ probed by stellar microlensing (**if** all of the DM is in extended PBH clusters containing $N_{\rm cl} = 10^3$ PBHs with mass $M_{\rm PBH} = 10^3 M_\odot$ constraint on $f_{\rm PBH}$ from long-duration microlensing survey weakens by ~10%). Petaĉ, Lavalle & Jedamzik; Gorton & Green.

Compact clusters

Local non-Gaussianity leads to enhanced clustering. Young & Byrnes

If clusters are sufficiently compact entire cluster (rather than individual PBHs) acts as single lens and microlensing constraints shifted to lower masses Calcino, Garcia-Bellido & Davis however other constraints (e.g. Lyman-α) are tightened. de Luca et al.

two-point correlator: $\xi_{\rm PBH} \approx \xi_0 \quad \text{for} \quad r \lesssim r_{\rm cl}$

excluded by microlensing, Lyman-α

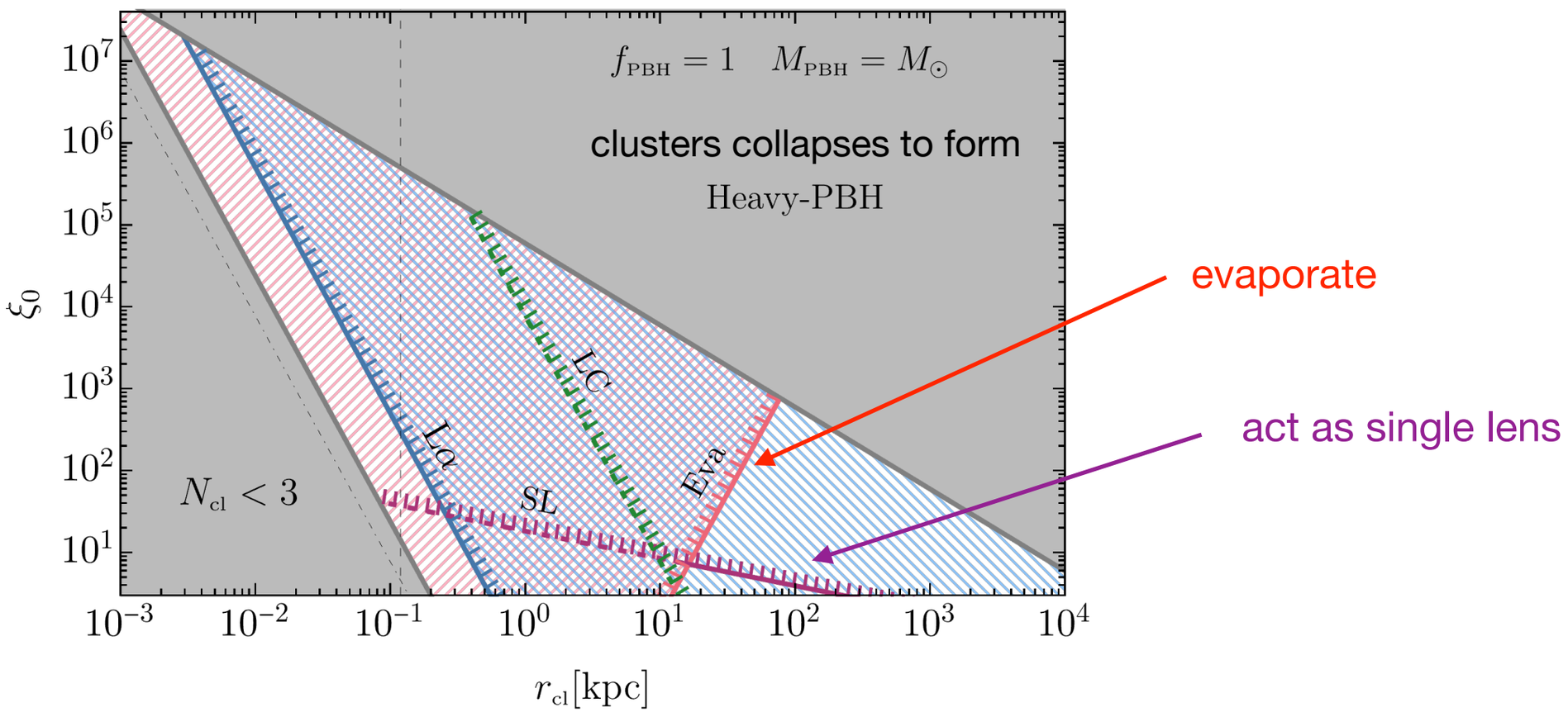

de Luca et al.

LMC microlensing constraints: MW density profile

Microlensing differential event rate depends on the spatial distribution of the lenses and also their velocity distribution:

Microlensing differential event rate

(assuming $f_{\rm PBH} = 1,\ M = 1 M_\odot$ & perfect detection efficiency)

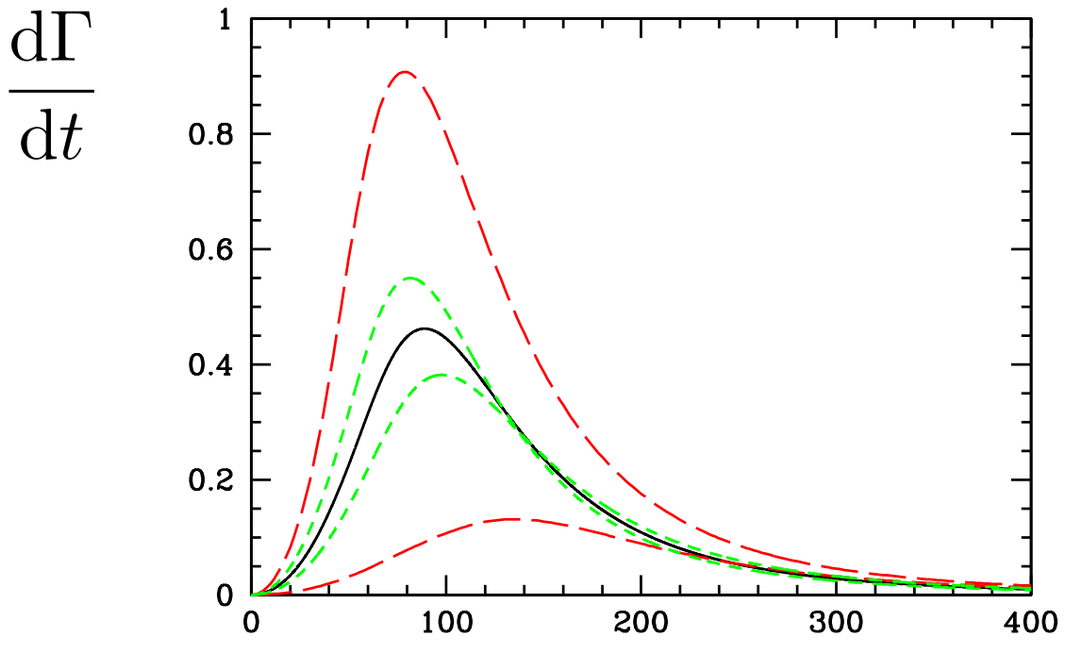

MW rotation curve

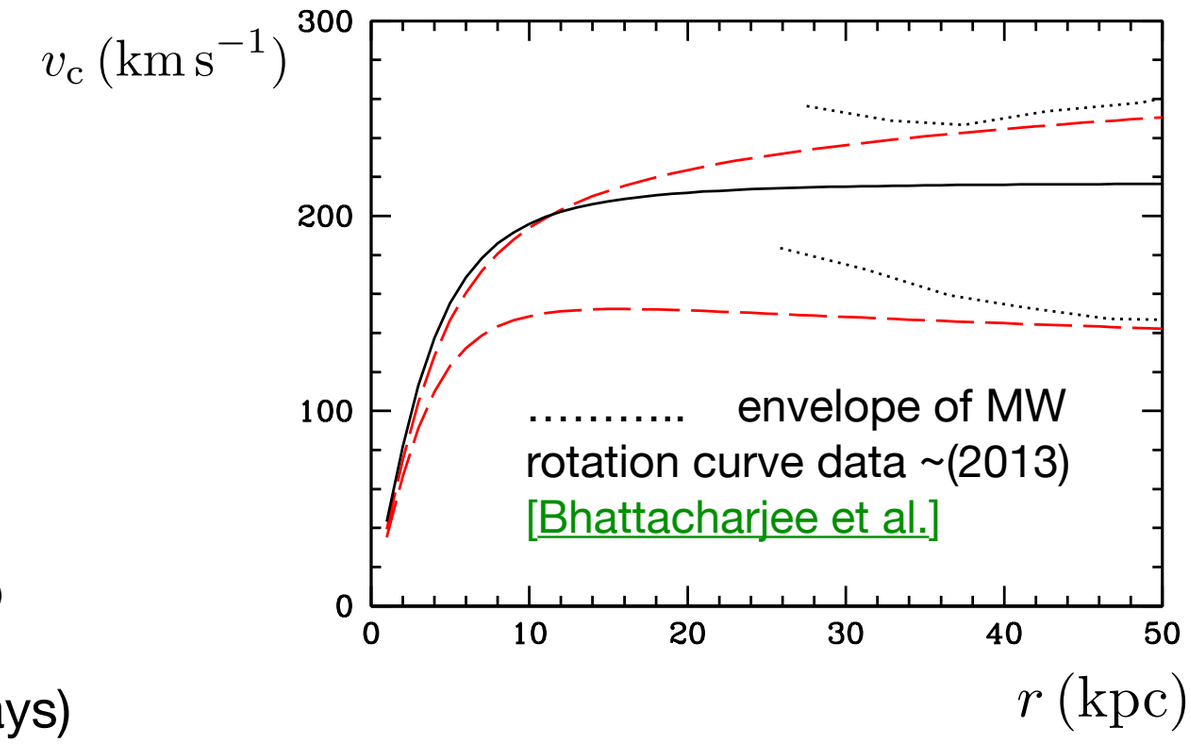

——— standard halo (SH), isothermal sphere, $\rho \propto r^{-2}$, flat rotation curve

— — — power law halos B (massive halo, rising rotation curve) and C (light halo, falling rotation curve)

- - - - - SH local circular speed, 200 & 240 km/s

Green (2017)

see also Alcock et al. (1996); Hawkins (2015); Calcino, Garcia-Bellido & Davis (2018); Garcia-Bellido & Hawkins (2024)

LMC microlensing constraints: MW density profile

Microlensing differential event rate depends on the spatial distribution of the lenses and their velocity distribution:

Microlensing differential event rate

(assuming $f_{\rm PBH} = 1,\ M = 1 M_\odot$ & perfect detection efficiency)

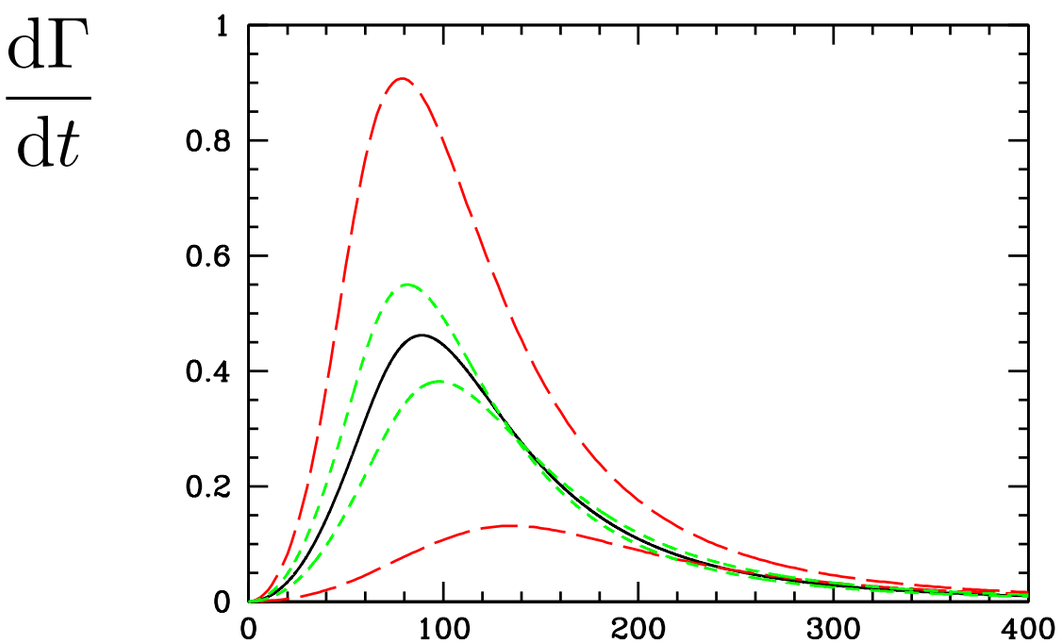

EROS constraints

(assuming delta-function MF)

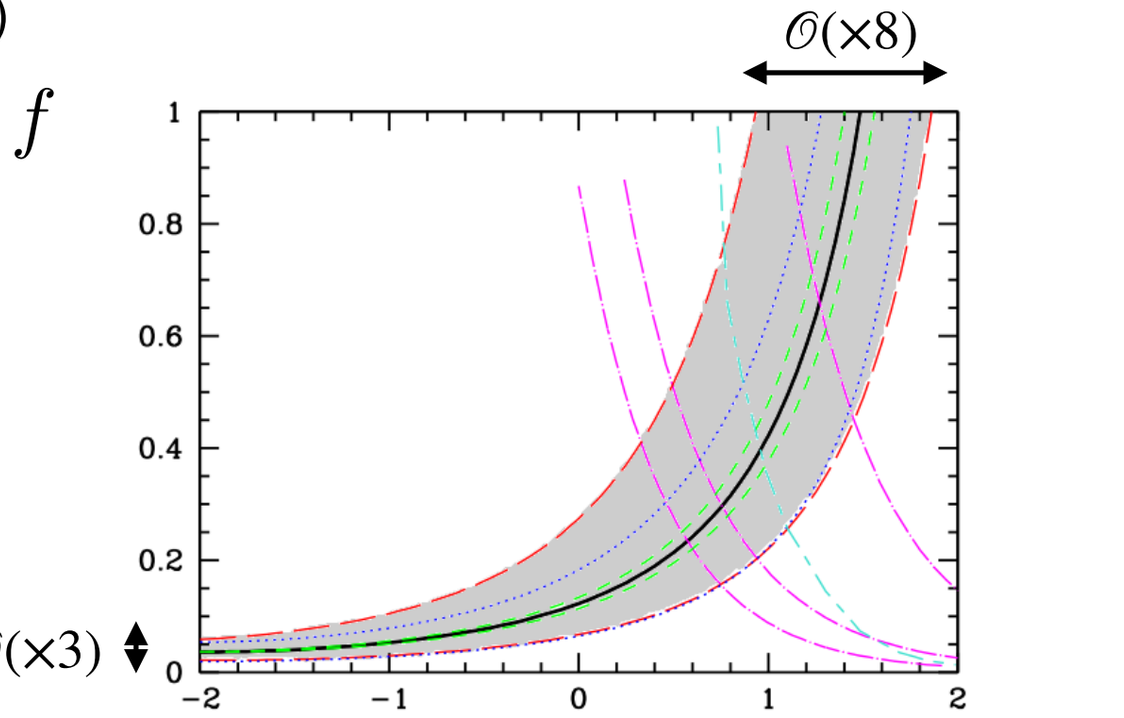

——— standard halo (SH), isothermal sphere, $\rho \propto r^{-2}$, flat rotation curve

— — — power law halos B (massive halo, rising rotation curve) and C (light halo, falling rotation curve)

- - - - - SH local circular speed, 200 & 240 km/s

..... SH local density, 0.005 and 0.015

Green (2017)

see also Alcock et al. (1996); Hawkins (2015); Calcino, Garcia-Bellido & Davis (2018); Garcia-Bellido & Hawkins (2024)

Falling MW rotation curve from *Gaia* DR3?

Three different studies using *Gaia* DR3 data find a declining MW rotation curve:

$$v_{\rm c}^2(R) = R \left.\frac{\partial \Phi}{\partial R}\right|_{z\approx 0}$$

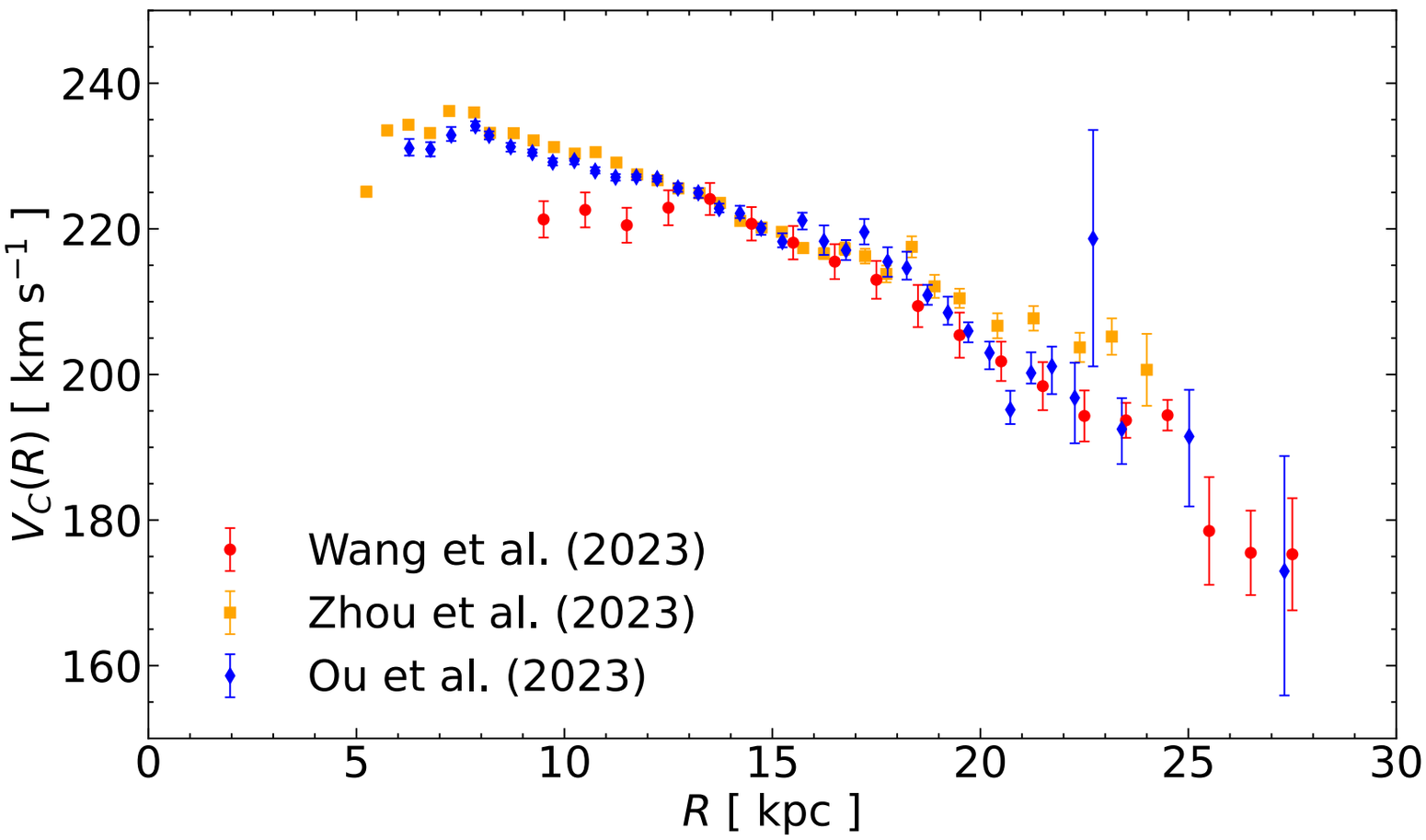

Jiao et al.

(Extrapolating to large R) gives significantly smaller MW halo mass ($0.2 \times 10^{12} M_\odot$) than from other tracers (stellar streams, globular clusters, MCs, dwarf galaxies): $(0.7 - 1.1) \times 10^{12} M_\odot$.

Analysis uses Jean's equations (found from taking velocity moments of collisionless Boltzmann equation), assumes MW is axisymmetric and in a steady state.

Also need to model density distribution of the tracer stars.

On the Galactic rotation curve inferred from the Jeans equations

Assessing its robustness using *Gaia* DR3 and cosmological simulations

Orlin Koop[1,⋆], Teresa Antoja[2], Amina Helmi[1], Thomas M. Callingham[1], and Chervin F. P. Laporte[2]

https://arxiv.org/abs/2405.19028

typical of galaxies that have been perturbed by external satellites. Also from the simulations we estimate that the difference between the true circular velocity curve and that inferred from Jeans equations can be as high as 15%, but that it likely is of order 10% for the Milky Way. This is of larger amplitude than the systematics associated to the observational uncertainties or those from most modelling assumptions when using the Jeans equations. However, if the density of the tracer population were truncated at large radii instead of being exponential as often assumed, this could lead to the erroneous conclusion of a steeply declining rotation curve.
Conclusions. We find that steady-state axisymmetric Jeans modelling becomes less robust at large radii, indicating that particular caution is needed when interpreting the rotation curve inferred in those regions. A more careful and sophisticated approach may be necessary for precision measurements of the dark matter content of our Galaxy.

Effect of declining rotation curve on OGLE-III + IV limits: Mroz et al. arXiv:2403.02386

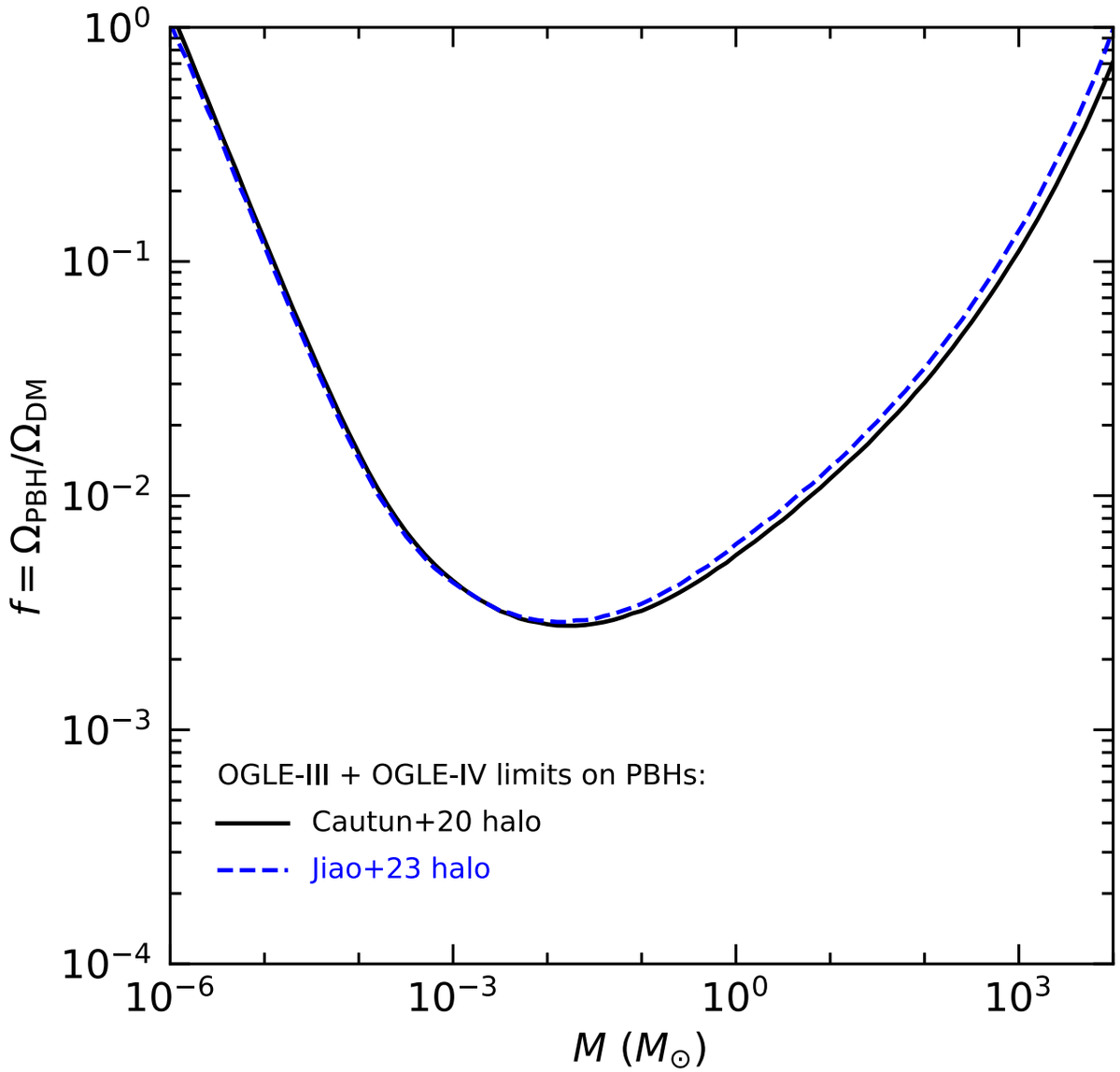

_____ Cautun et al. MW mass model fitted to *Gaia* DR2 rotation curve + other data., halo with contracted NFW profile (motivated by hydro simulations including baryons).

- - - - - - - - - Jiao et al. MW mass model fitted to declining *Gaia* DR3 rotation curve, halo with Einasto profile.

3. How open is the asteroid mass window?

Due to critical collapse BH mass depends on size of fluctuation it forms from:

$$M = kM_{\mathrm{H}}(\delta - \delta_{\mathrm{c}})^{\gamma}$$

M_{H} = horizon mass, δ = density contrast, δ_c = threshold for collapse,
$\gamma = 0.36$ & k constants

Even if all PBHs form at the same time (i.e. from a narrow peak in the power spectrum) they won't all have the same mass. Niemeyer & Jedamzik

Critical collapse mass function:

(assumes probability distribution of δ is gaussian)

$$\psi(M_{\mathrm{PBH}}) \equiv \frac{1}{\rho}\frac{\mathrm{d}\rho}{\mathrm{d}M_{\mathrm{PBH}}} \propto \left(\frac{M_{\mathrm{PBH}}}{M_{\mathrm{p}}}\right)^{1/\gamma} \exp\left[-\left(\frac{M_{\mathrm{PBH}}}{M_{\mathrm{p}}}\right)^{1/\gamma}\right]$$

Generalised critical collapse mass function: Gow et al.

$$\psi(M_{\mathrm{PBH}}) \propto \left(\frac{M_{\mathrm{PBH}}}{M_{\mathrm{p}}}\right)^{\alpha} \exp\left[-\frac{\alpha}{\beta}\left(\frac{M_{\mathrm{PBH}}}{M_{\mathrm{p}}}\right)^{\beta}\right]$$

For extended mass functions (MFs), constraints on f_{PBH} are smeared out, and gaps between constraints are ‘filled in’: Green; Carr et al.

monochromatic

log-normal
(fixed width)

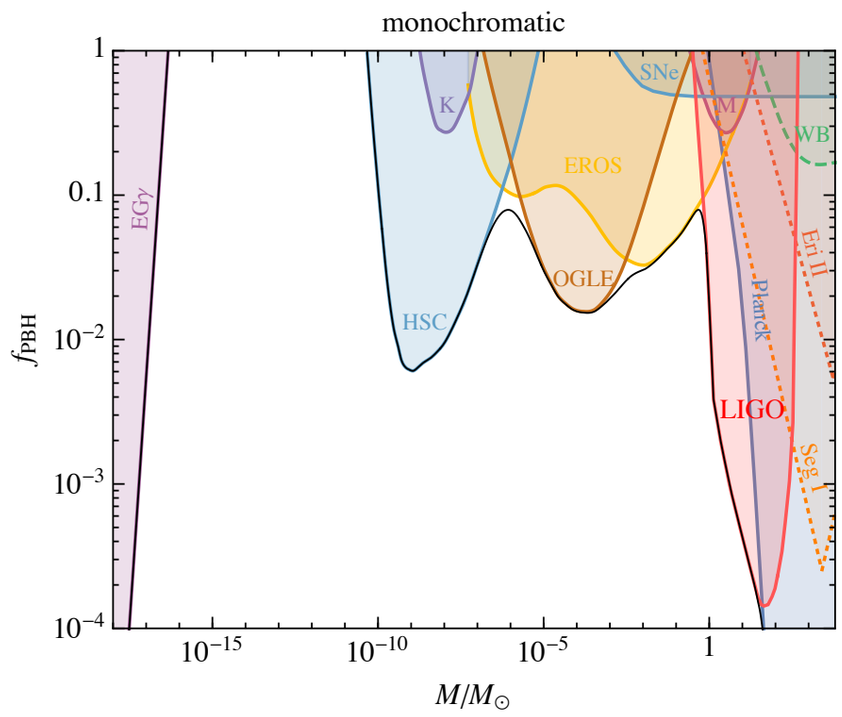

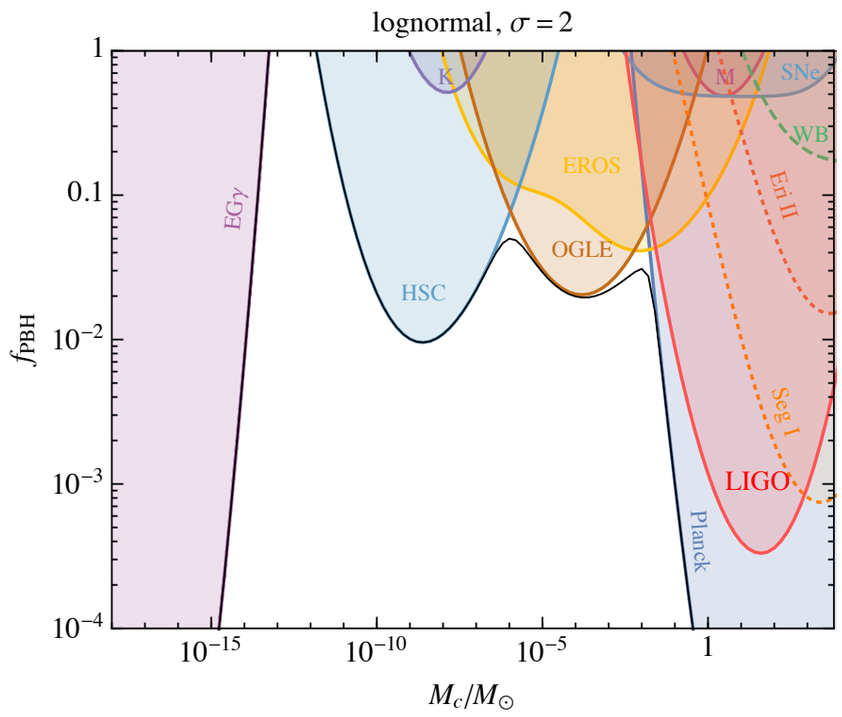

$\frac{M_c}{M_\odot}$

Carr et al.

However:

The tails of the PBH MF are not well-fit by a lognormal Gow et al.,

How far the evaporation and microlensing constraints extend into the asteroid mass window ($10^{17}\,\mathrm{g} \lesssim M_{\rm PBH} \lesssim 10^{22}\,\mathrm{g}$) depends on the shape of the low and high mass tails, respectively, of the MF.

best fit MFs from a lognormal peak in the power spectrum Gow et al.

narrow

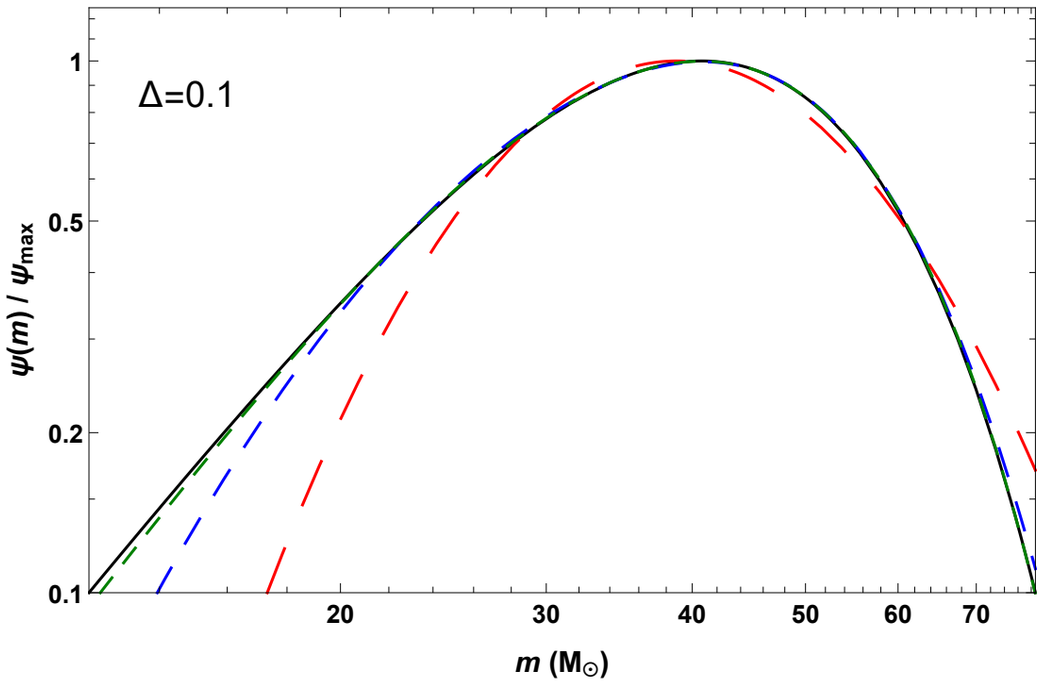

broad

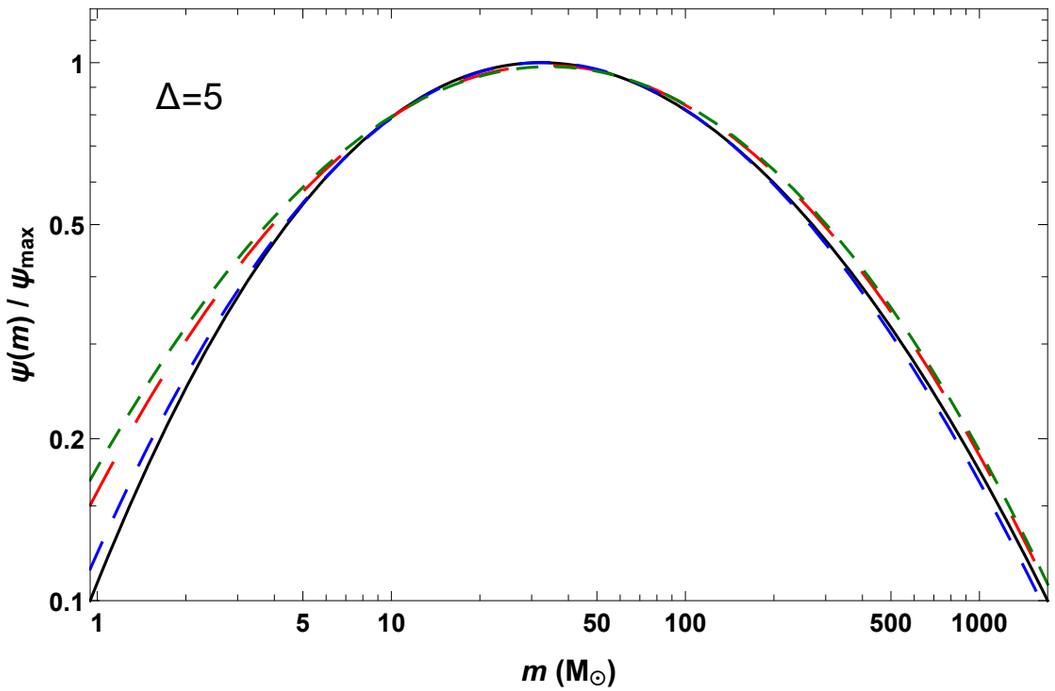

- - - - - - - - generalised critical collapse - - - - - - skew lognormal __ __ __ __ lognormal

Narrow peak ($\Delta \lesssim 0.5$): critical collapse dominates & generalised critical collapse MF is best fit.

Broad peak: width of the power spectrum is important & skew lognormal is best fit.

(Power spectrum produced by hybrid inflation with a mild waterfall transition Clesse & Garcia-Bellido is well fit by lognormal with $\Delta = 5$.)

Constraints for best fit MF from a broad ($\Delta = 5$) peak in the power spectrum

____ delta-function, …. lognormal _._._ skew lognormal

current

Voyager 1 $e^{\pm}$ Boudaud & Cirelli

MeV gamma rays Korwar & Profumo

Subaru-HSC M31 microlensing Niikura et al.; Croon et al.

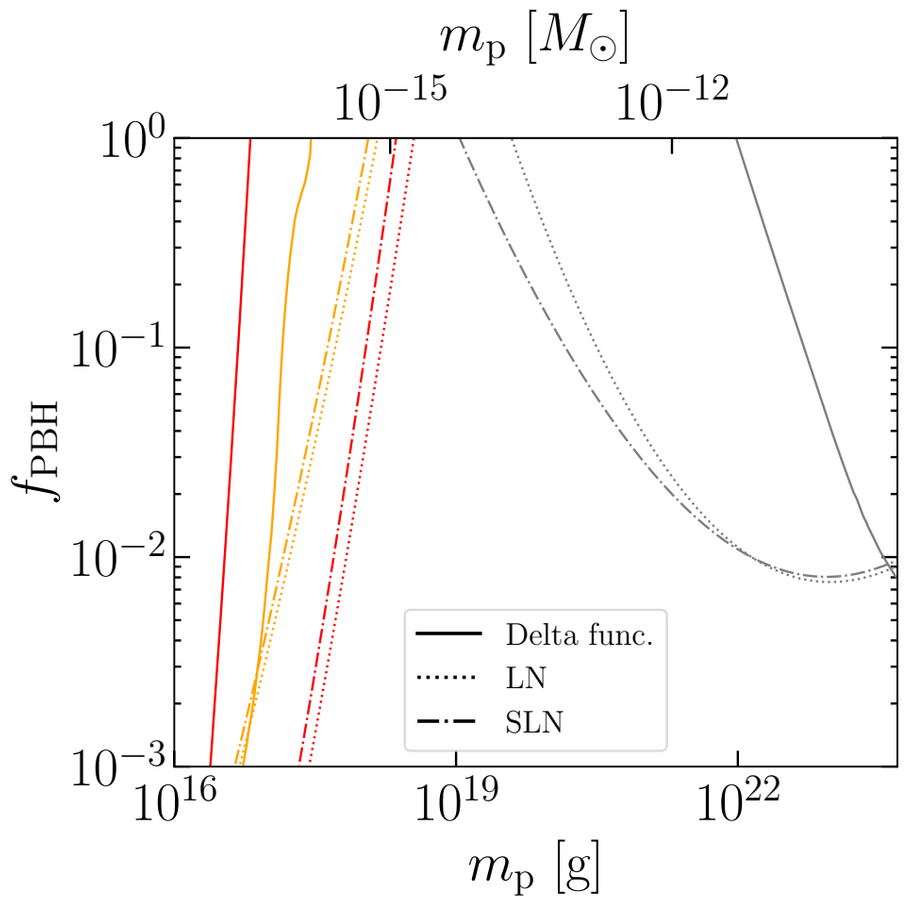

future (+ Voyager 1 $e^{\pm}$)

MeV gamma rays Coogan et al.

microlensing LMC white dwarfs Sugiyama et al.

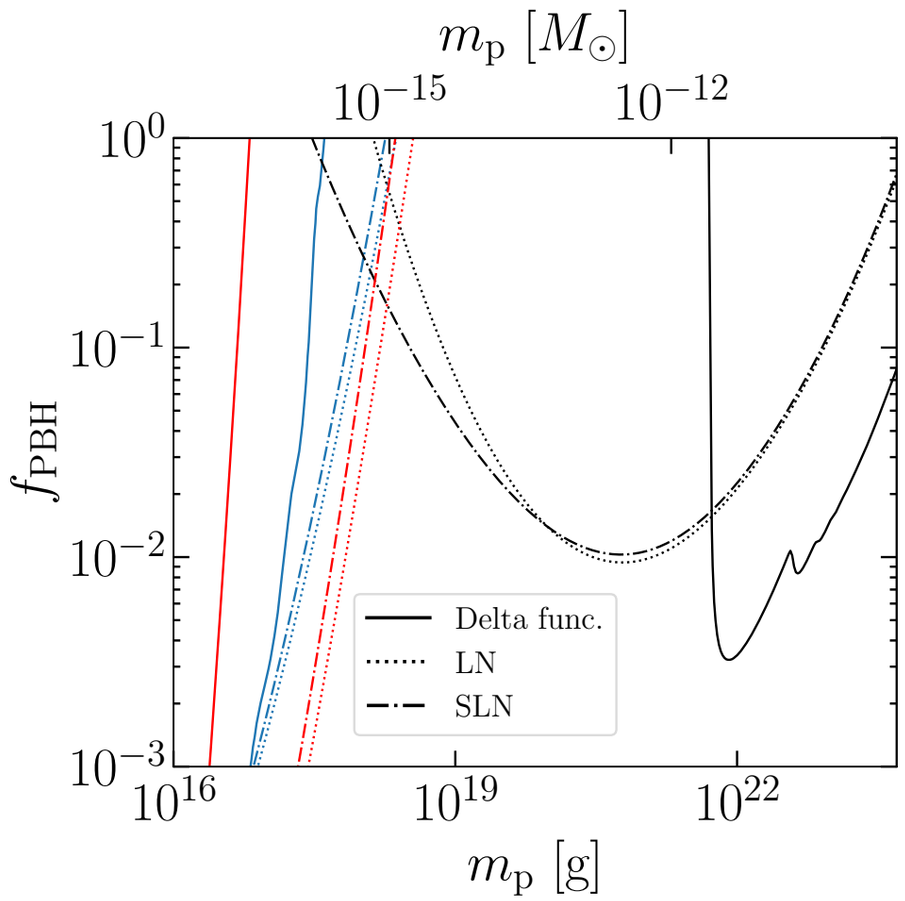

Gorton & Green

Summary

- Various **microlensing** observations (stars in LMC, supermagnified stars, flux ratios of multiple lensed quasars) lead to $f_{\rm PBH} \lesssim \mathcal{O}(10^{-2})$ for $10^{-4} M_\odot \lesssim M_{\rm PBH} \lesssim 100 M_\odot$ (under 'standard' assumptions about DM distribution).

- **Clusters** formed due to initial Poissonian fluctuations in PBH distribution are sufficiently extended that PBHs microlens individually.
  Change in stellar microlensing constraints is small.
  Non-gaussianity can lead to compact clusters: microlensing constraints shifted to smaller PBH masses, but Lyman-α constraints tightened.

- **Stellar microlensing constraints** depend on DM density and velocity distribution.
  uncertainty in tightest value of constraint on $f_{\rm PBH}$: $\mathcal{O}(2-3)$,
  uncertainty in mass for which $f_{\rm PBH} = 1$: $\mathcal{O}(10)$

- Range of masses over which a constraint gives $f_{\rm PBH} < 1$ depend on **shapes of tails of MF.**
  'Asteroid mass window' currently open even for MFs from broad peaks in power spectrum.

Back-up slides

Differential event rate,
assuming a delta-function lens mass function and a spherical halo with a Maxwellian velocity distribution (and neglecting the transverse velocity of the microlensing tube): [Griest]

$$\frac{\mathrm{d}\Gamma}{\mathrm{d}\hat{t}} = \frac{32 L u_{\mathrm{T}}^4}{\hat{t}^4 M v_{\mathrm{c}}^2} \int_0^1 \rho(x)\, R_{\mathrm{E}}^4(x)\, \exp\left[-\frac{4R_{\mathrm{E}}^2(x)}{\hat{t}^2 v_{\mathrm{c}}^2}\right] \mathrm{d}x$$

$\rho(x)$ = compact object density distribution

$\hat{t}$ = Einstein ***diameter*** crossing time (as used by the MACHO collab., EROS & OGLE use Einstein radius crossing time)

v_c = local circular speed (usually taken to be 220 km/s, ~10s% uncertainty)

Expected number of events:

$$N_{\mathrm{exp}} = E \int_0^\infty \frac{\mathrm{d}\Gamma}{\mathrm{d}\hat{t}}\, \epsilon(\hat{t})\, \mathrm{d}\hat{t}$$

E = exposure (number of stars times duration of obs.)

$\epsilon(\hat{t})$ = efficiency (prob. that an event of duration $\hat{t}$ is observed)

Standard halo model

cored isothermal sphere:

$$\rho(r) = \rho_0 \frac{R_c^2 + R_0^2}{R_c^2 + r^2}$$

$\rho_0 = 0.008\, M_\odot\, \mathrm{pc}^{-3}$, local dark matter density

$R_c = 5\,\mathrm{kpc}$, core radius

$R_0 = 8.5\,\mathrm{kpc}$, Solar radius

‘Backgrounds’

i) variable stars, supernovae in background galaxies

cuts/fits developed to eliminate them (but some events only rejected years later, after star’s brightness varied a 2nd time!)

ii) lensing by stars in MW or Magellanic Clouds themselves (‘self-lensing’)

model and include in event rate calculation

Differential event rate for $M = 1\,M_\odot$ and halo fraction f=1:
($\hat{t} \propto M^{1/2}$, $\quad \mathrm{d}\Gamma/\mathrm{d}\hat{t} \propto M^{-1}$)

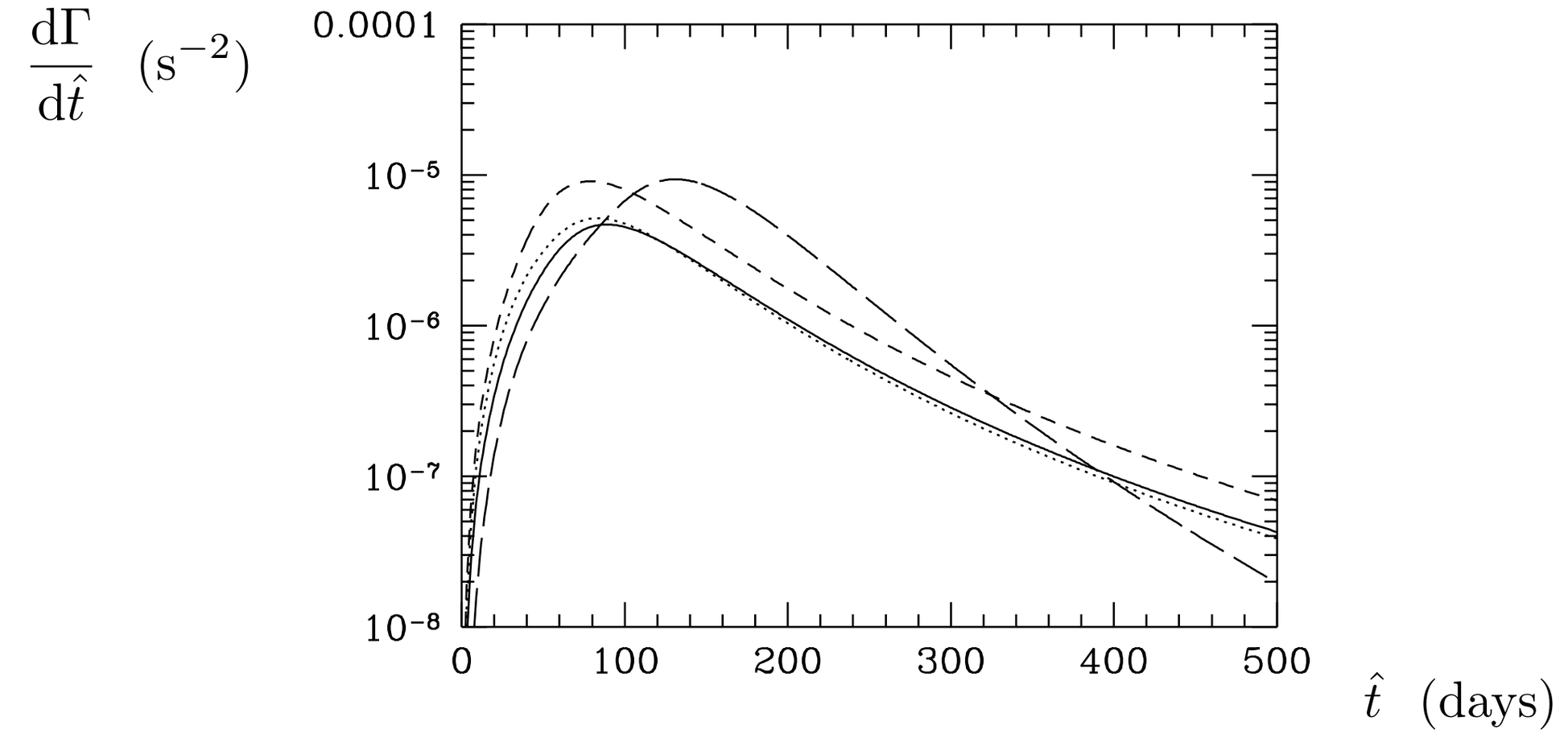

_____ = standard halo model

. . . . . = standard halo model including transverse velocity

- - - - = Evans power law model: massive halo with rising rotation curve, $v_\mathrm{c} \propto R^{0.2}$

_ _ _ _ = Evans power law model: flattened halo with falling rotation curve, $v_\mathrm{c} \propto R^{-0.2}$

velocity anisotropy can affect rate at ~10% level [De Paolis, Ingrosso & Jetzer]

Observations

MACHO

Monitored 12 million stars in LMC for 5.7 years.

Found 13/17 events (for selection criteria A/B, B less restrictive-picks-up exotic events).

Detection efficiency

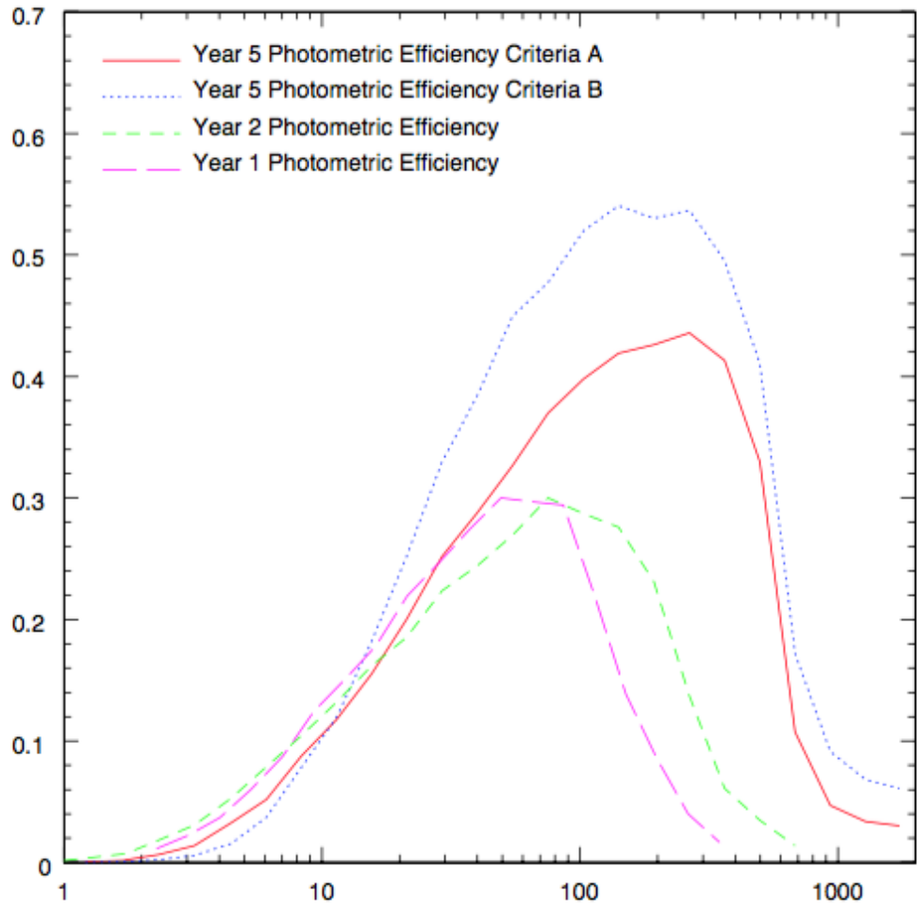

5 years A
5 years B
2 years
1 year

BUT

LMC-5: lens identified (using HST obs & parallax fit) as a low mass MW disc star. [MACHO]

LMC-9: (only satisfied criteria B) lens is a binary, allowing measurement of low projected velocity, which suggests lens is in LMC (or source is also binary). [MACHO]

LMC-14: source is binary, and lens most likely to lie in LMC. [MACHO]

LMC-20: (only satisfied criteria B) lens identified (using Spitzer obs) as a MW thick disc star. [Kallivayalil et al.]

LMC-22: (only satisfied criteria B) supernova or an AGN in background galaxy. [MACHO]

LMC-23: varied again, so not microlensing [EROS/OGLE]

EROS

Monitored 67 million stars in LMC and SMC for 6.7 years.

Use bright stars in sparse fields (to avoid complications due to ‘blending’-contribution to baseline flux from unresolved neighbouring star).

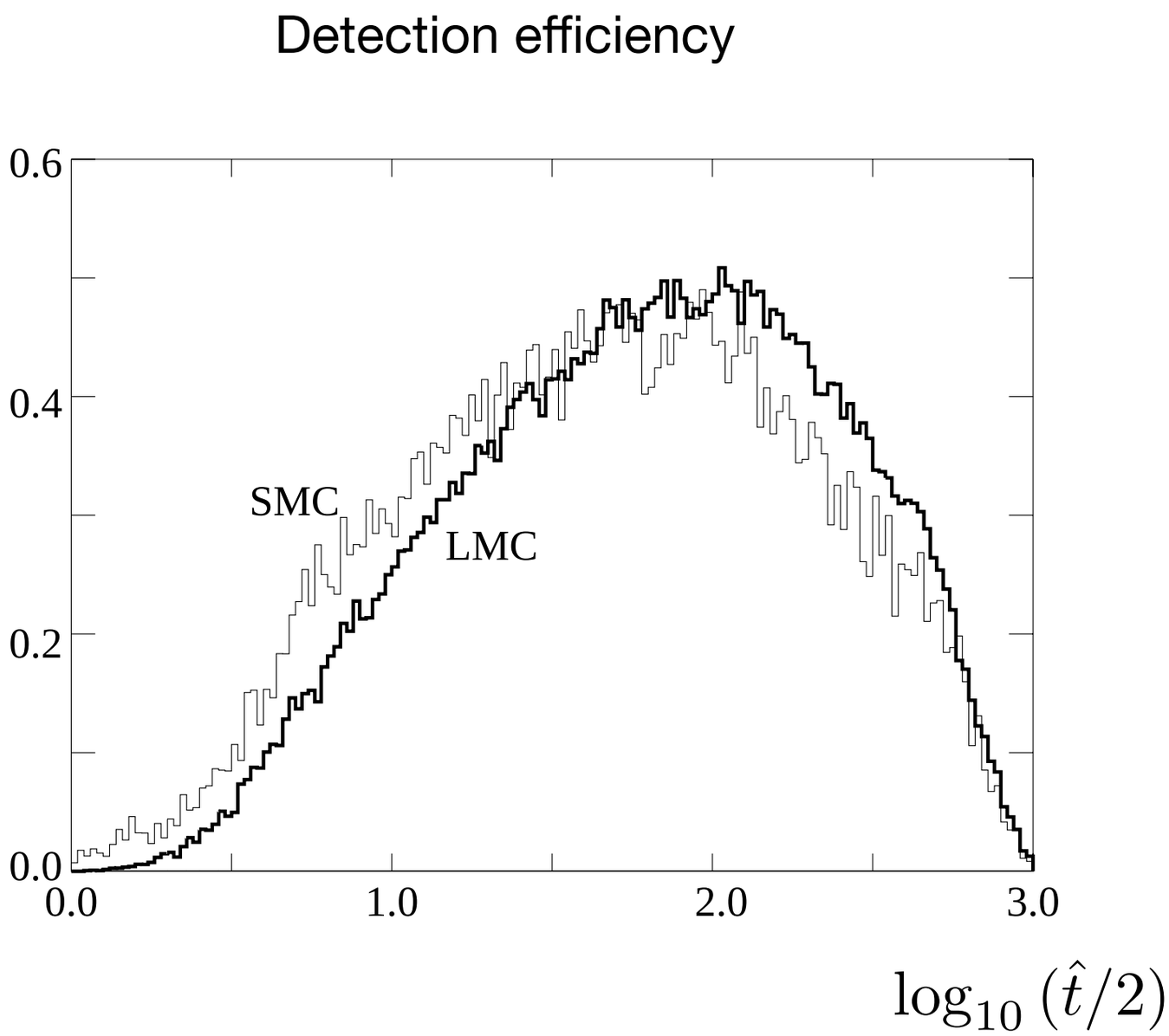

Final result: 1 SMC event (also seen by MACHO collab.) consistent (number & duration) with expectations for self-lensing (SMC is aligned along line of sight). [Graff & Gardiner]

Earlier candidate events eliminated: 7 varied again and 3 identified as supernovae.

Constraints on fraction of halo in compact objects, f,
(assuming a delta-function mass function):

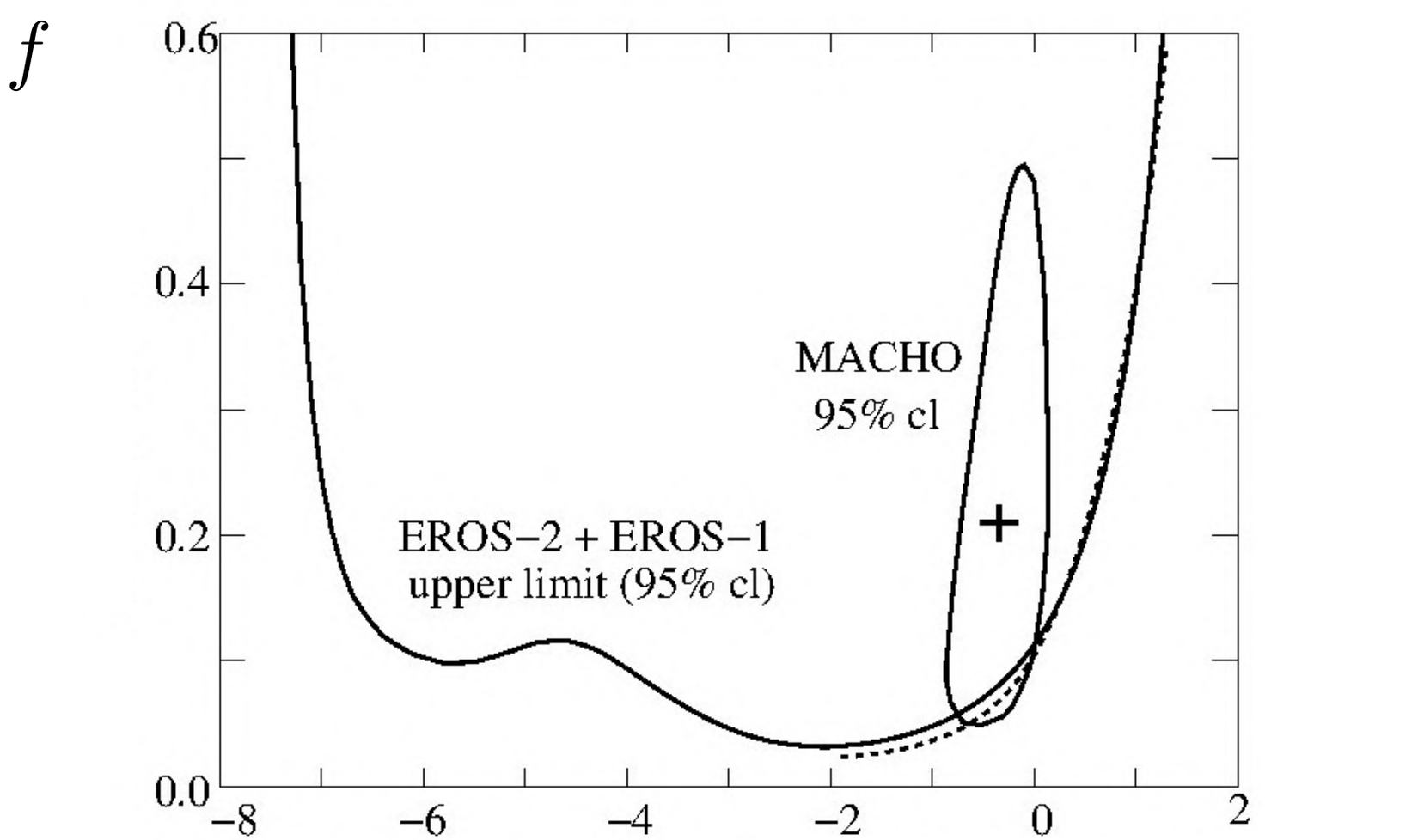

EROS

Phase space distribution function: $f(\mathbf{x}, \mathbf{v}, t)$

Number of particles with phase space co-ordinates in $\mathbf{x} \rightarrow \mathbf{x} + \mathrm{d}\mathbf{x}$ and $\mathbf{v} \rightarrow \mathbf{v} + \mathrm{d}\mathbf{v}$ at time t: $f(\mathbf{x}, \mathbf{v}, t)\mathrm{d}^3\mathbf{x}\mathrm{d}^3\mathbf{v}$

Steady-state phase space distribution of a collection of collisionless particles is given by the solution of the collisionless Boltzmann equation:

$$\frac{\mathrm{d}f}{\mathrm{d}t} = 0$$

in Cartesian co-ordinates:

$$\frac{\partial f}{\partial t} + \mathbf{v}.\frac{\partial f}{\partial \mathbf{x}} + \frac{\partial \Phi}{\partial \mathbf{x}}.\frac{\partial f}{\partial \mathbf{v}} = 0$$

Poisson's equation for a self-consistent system (where density distribution generates potential):

$$\nabla^2\Phi = 4\pi G\rho = 4\pi G \int f \mathrm{d}^3\mathbf{v}$$

A solution is:

$$\rho(r) = \frac{\sigma^2}{2\pi G r^2} \qquad f \propto \exp(-v^2/2\sigma^2)$$

c.f. the phase-space distribution of a self-gravitating isothermal sphere with

$$\sigma^2 = k_\mathrm{B}T/m$$

Collisionless particles can change their energy & reach the steady-state configuration if they experience a fluctuating gravitational potential (violent relaxation). However real DM halos haven't reached a steady state and contain substructure (subhalos and streams).

Local circular speed e.g:

Reid et al. proper motion of Sgr A*:

$$v_c(R_\odot)/R_\odot = (30.3 \pm 0.9)\,\mathrm{km\,s^{-1}\,kpc^{-1}}$$

and using new precise measurement of $R_\odot$ gives

$$v_c(R_\odot) = (248 \pm 7)\,\mathrm{km\,s^{-1}\,kpc^{-1}}$$

Eilers et al. Jeans analysis from taking moment of collision less Boltzmann equations (in cylindrical co-cordinates):

$$v_c^2(R) = R\frac{\partial \Phi}{\partial R}_{z\approx 0} = \langle v_\phi^2 \rangle - \langle v_R^2 \rangle \left(1 + \frac{\partial \ln \nu}{\partial \ln R} + \frac{\partial \ln \langle v_R^2 \rangle}{\partial \ln R}\right)$$

ν = density of tracer stars.

combing data from Gaia, APOGEE and other sources:

$$v_c(R_\odot) = (229.0 \pm 0.2)\,\mathrm{km\,s^{-1}}$$

with (2-5)% systematic uncertainty (from e.g. uncertainty in distribution of tracer stars).

n.b. Standard halo has one-to-one relationship between circular speed and velocity dispersion & peak speed, but in general this isn't the case.

Clustering of PBHs formed from collapse of large density perturbations

PBHs don't form in clusters Ali-Haïmoud (previous work Chisholm extrapolated an expression for the correlation function beyond its range of validity).

However there are additional isocurvature perturbations (due to Poisson fluctuations in PBH distribution) and PBH clusters form shortly after matter-radiation equality.
Afshordi, Macdonald & Spergel; Inman & Ali-Haïmoud; Jedamzik

power spectrum

$P(k)$

$(\propto k^{n_s})$

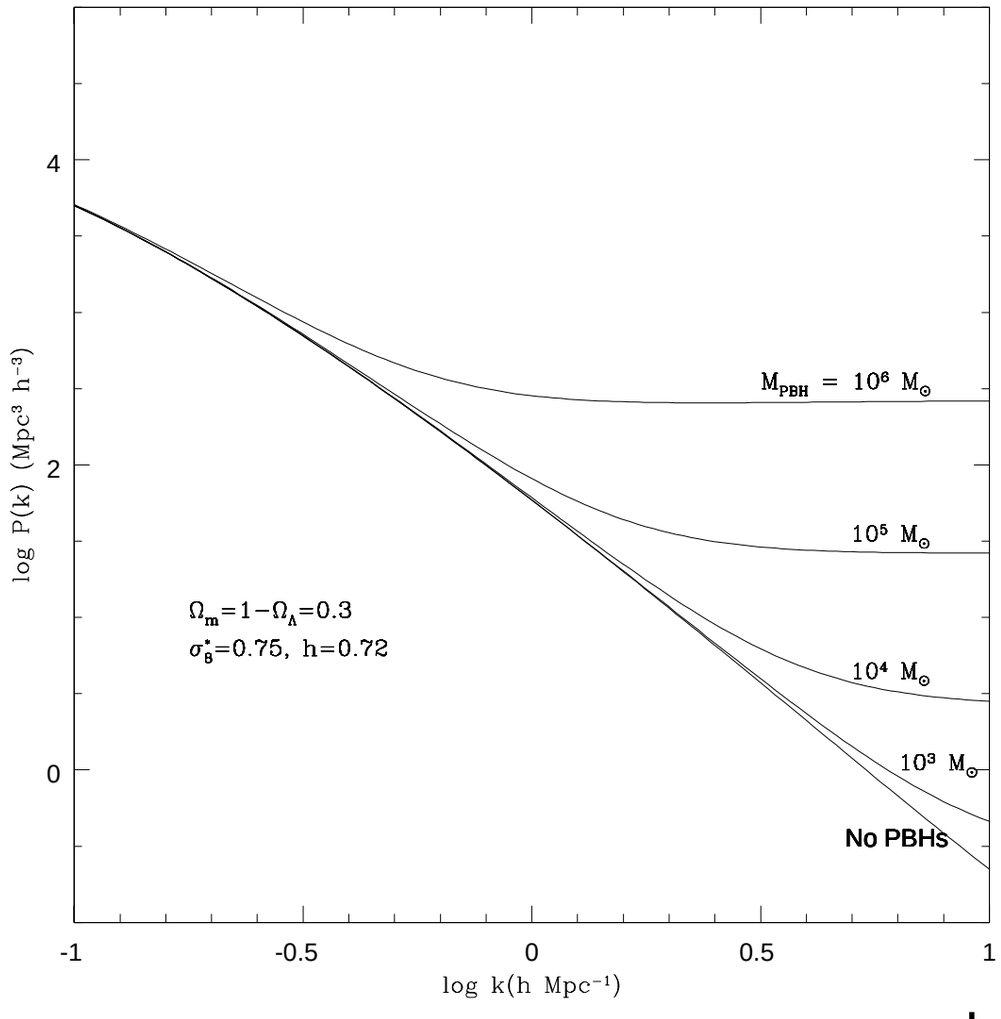

increasing PBH mass

no PBHs

k = comoving wavenumber

Afshordi, Macdonald & Spergel

Clustering of PBHs formed from collapse of large density perturbations

PBHs don't form in clusters Ali-Haïmoud (previous work Chisholm extrapolated an expression for the correlation function beyond its range of validity).

However there are additional isocurvature perturbations (due to Poisson fluctuations in PBH distribution) and PBH clusters form shortly after matter-radiation equality.
Afshordi, Macdonald & Spergel; Inman & Ali-Haïmoud; Jedamzik

mass variance

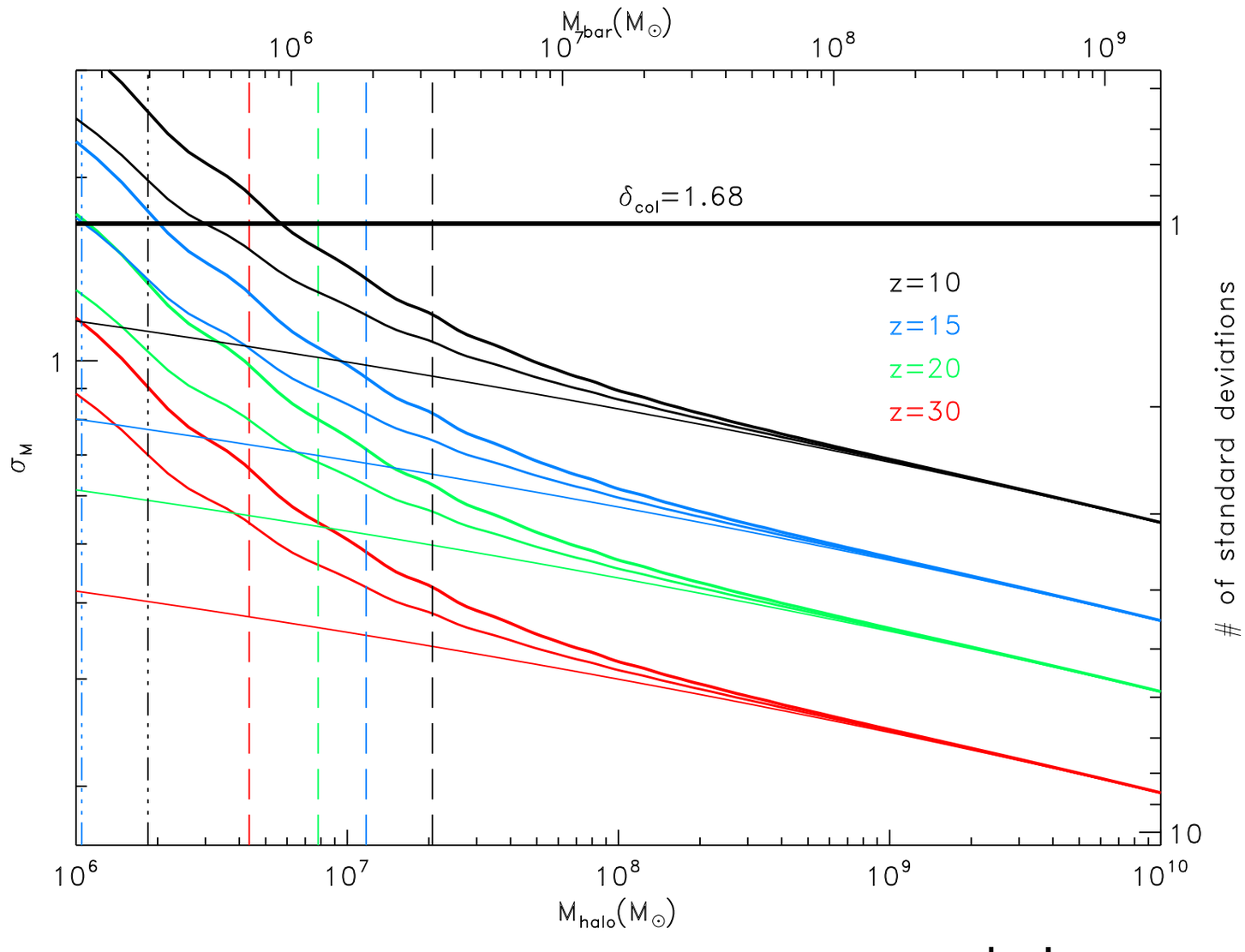

halo mass

Kashlinksy

← threshold for collapse

z= 10, 15, 20, 30

M_{PBH}=30 $M_\odot$

M_{PBH}=15 $M_\odot$

no PBHs

Approximate analytic calculation

c.f. Afshordi, Macdonald & Spergel; Jedamzik

PBH DM has additional isocurvature perturbations due to Poisson fluctuations in their distribution:

$$\delta(N) = \frac{\Delta N}{N} = \frac{1}{\sqrt{N}}$$

growth factor for isocurvature perturbations:

$$D(a) \approx \left(1 + \frac{3}{2}\frac{a}{a_{\rm eq}}\right)$$

spherical top hat collapse:

collapse occurs when:

$$D(a_{\rm col})\delta(N) = \delta_{\rm critical} \approx 1.69$$

final halo/cluster density:

$$\rho_{\rm cl} \approx 178\rho_{\rm DM}(a_{\rm coll})$$

radius of cluster:

$$r_{\rm cl} \approx 0.01\left(\frac{M_{\rm PBH}}{M_\odot}\right)^{1/3} N^{5/6}\,{\rm pc}$$

For $M_{\rm PBH} = M_\odot$, N=10 (100) clusters form at $z_{\rm coll}$ ≈1200 (320) and have $r_{\rm cl}$≈ 0.06 (0.5) pc.

N-body simulations

Inman & Ali-Haïmoud

Simulate a L = 30 h^{-1} kpc box, with $M_{\rm PBH} = 20 h^{-1} M_\odot$ from radiation domination to z = 99, for $f_{\rm PBH} = 1$ and also $f_{\rm PBH} < 1$ + particle dark matter.

matter field at z=100

$f_{\rm PBH} = 10^{-5}$

a PBH!

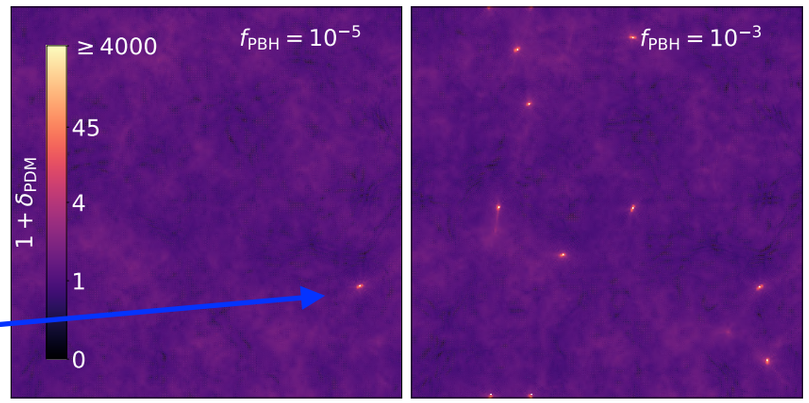

$f_{\rm PBH} = 10^{-3}$

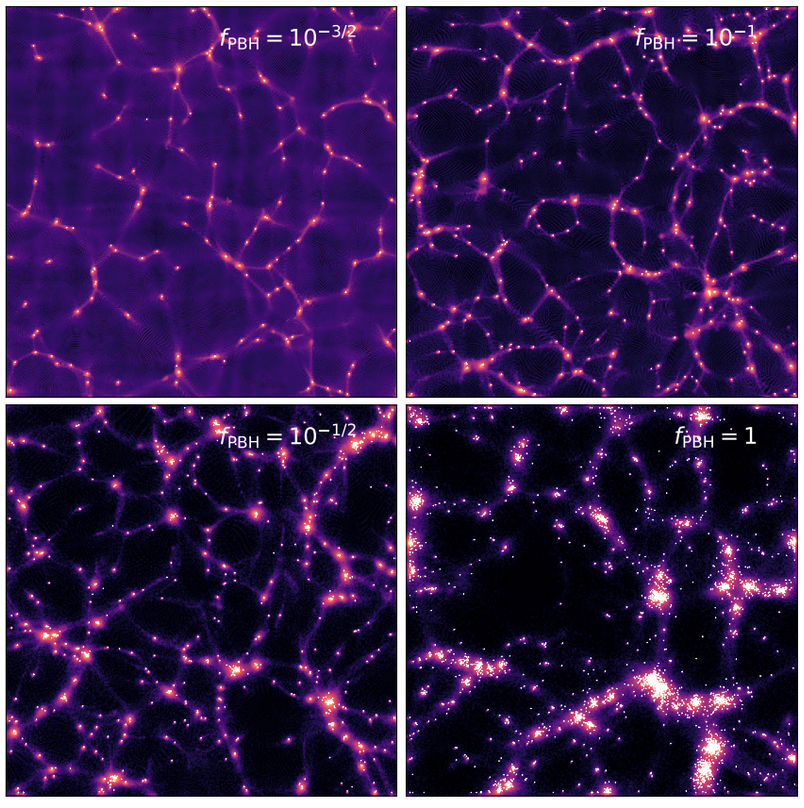

$f_{\rm PBH} = 10^{-3/2}$

$f_{\rm PBH} = 10^{-1}$

$f_{\rm PBH} = 10^{-1/2}$

$f_{\rm PBH} = 1$

Inman & Ali-Haïmoud

Clusters containing small numbers of PBHs always most abundant, but abundance of clusters containing large numbers of PBHs increases with time.

halo mass function (number of halos containing a given number of PBHs)

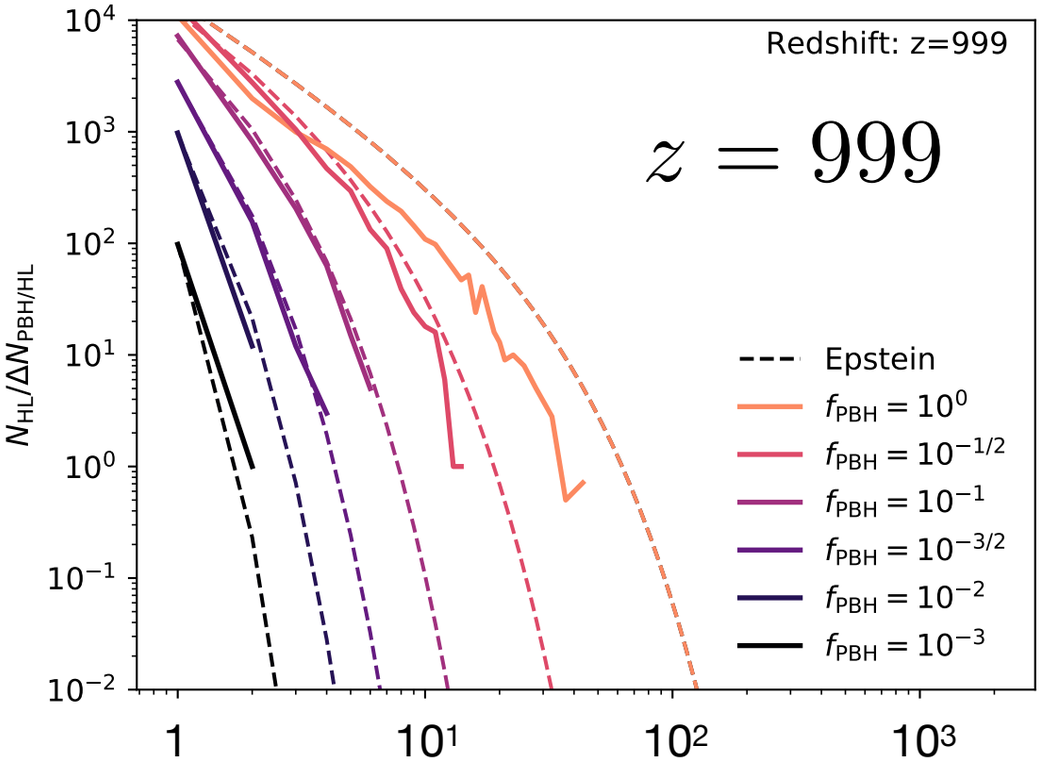

decreasing f_{PBH}

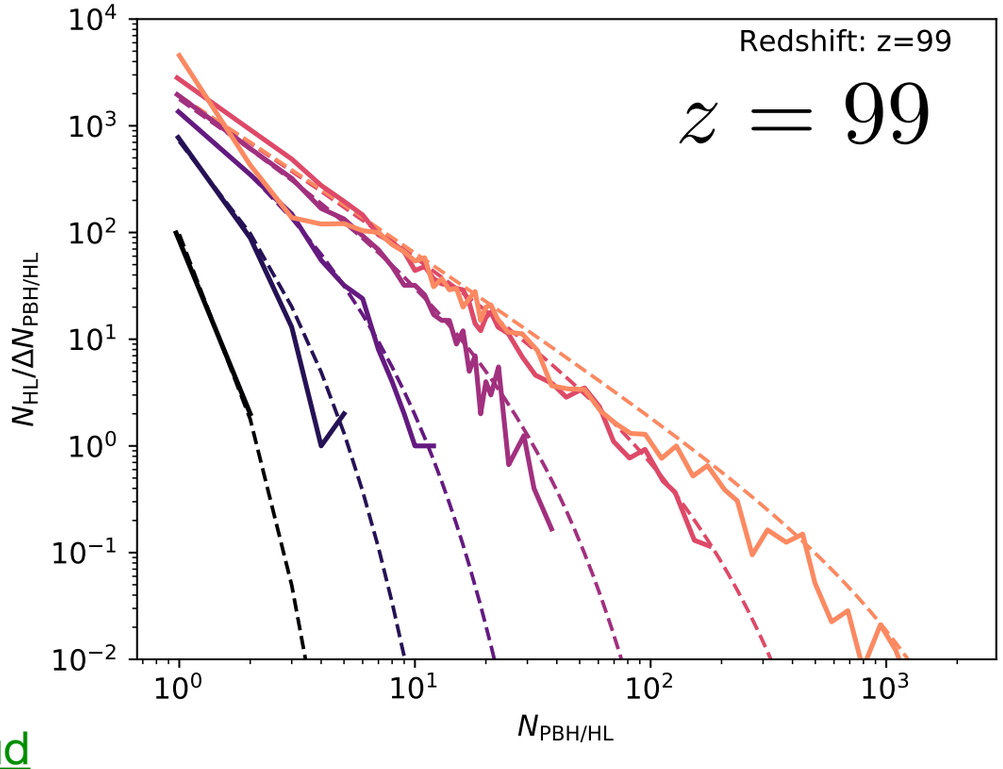

Inman & Ali-Haïmoud

Evolution of PBH clusters (and in particular PBH binaries) through to the present day is a challenging open problem. e.g. Jedamzik; Trashorras et al….

Clusters containing $\lesssim 10^3$ PBHs will evaporate by present day. Afshordi, Macdonald & Spergel; Jedamzik

Effect of clustering on LMC microlensing constraints

Gorton & Green (see also Petaĉ, Lavalle & Jedamzik)

For PBHs formed from collapse of density perturbations during radiation, clusters are sufficiently extended that PBHs lens individually (separation of PBHs $\gg R_E$).

Microlensing from a single cluster:

looking down on line of sight

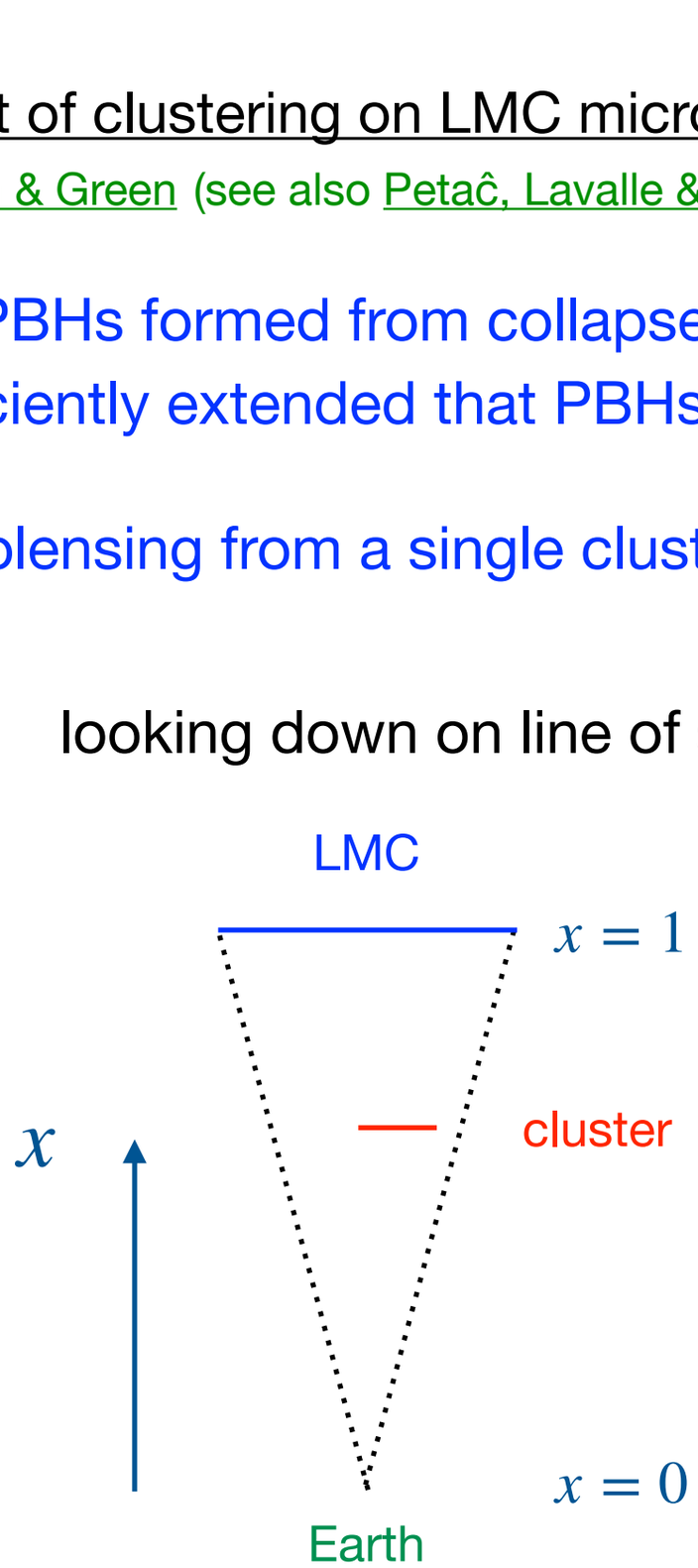

x = fractional line of sight dist

looking along line of sight

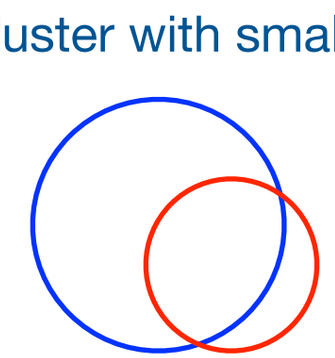

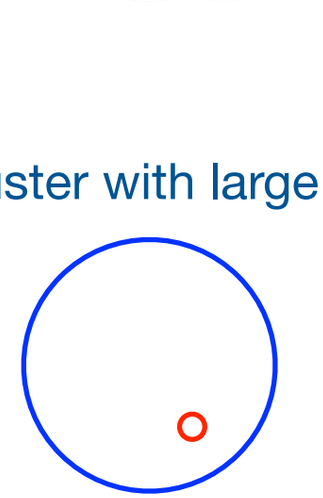

probability of finding a cluster at line of sight distance x is proportional to cross sectional area of 'cone' to LMC $\propto x^2$

all the PBHs in a given cluster cause events with the same duration:

$$\hat{t} = \frac{2R_{\rm E}(x)}{v} \propto [x(1-x)]^{1/2}$$

rate at which cluster causes microlensing events is proportional to solid angle subtended by cluster times Einstein radius:

$$\propto \frac{[x(1-x)]^{1/2}}{x^2}$$

Close clusters (small x) are rare, but if one intersects the line of sight if produces short duration events at a high rate.

n.b. Germani and Sheth have calculated MF of PBHs, using the statistics of the compaction function.

Find low mass tail generically $\psi(m) \propto m^{1/\gamma}$, high mass tail has cutoff which depends on shape & amplitude of power spectrum.